

# Epac2-dependent mobilization of intracellular $\text{Ca}^{2+}$ by glucagon-like peptide-1 receptor agonist exendin-4 is disrupted in $\beta$ -cells of phospholipase C- $\epsilon$ knockout mice

Igor Dzhura<sup>1</sup>, Oleg G. Chepurny<sup>1</sup>, Grant G. Kelley<sup>1,2</sup>, Colin A. Leech<sup>1</sup>, Michael W. Roe<sup>1,3</sup>, Elvira Dzhura<sup>1</sup>, Parisa Afshari<sup>2</sup>, Sundeep Malik<sup>4</sup>, Michael J. Rindler<sup>5</sup>, Xin Xu<sup>6</sup>, Youming Lu<sup>6</sup>, Alan V. Smrcka<sup>4</sup> and George G. Holz<sup>1,2</sup>

Departments of <sup>1</sup>Medicine, <sup>2</sup>Pharmacology and <sup>3</sup>Cell Biology and Developmental Biology, State University of New York Upstate Medical University, Syracuse, NY, USA

<sup>4</sup>Department of Pharmacology and Physiology, University of Rochester School of Medicine, Rochester, NY, USA

<sup>5</sup>Department of Cell Biology, New York University School of Medicine, New York, NY, USA

<sup>6</sup>Departments of Neurology and Neuroscience, Louisiana State University, Health Science Center, School of Medicine, New Orleans, LA, USA

Calcium can be mobilized in pancreatic  $\beta$ -cells via a mechanism of  $\text{Ca}^{2+}$ -induced  $\text{Ca}^{2+}$  release (CICR), and cAMP-elevating agents such as exendin-4 facilitate CICR in  $\beta$ -cells by activating both protein kinase A and Epac2. Here we provide the first report that a novel phosphoinositide-specific phospholipase C- $\epsilon$  (PLC- $\epsilon$ ) is expressed in the islets of Langerhans, and that the knockout (KO) of PLC- $\epsilon$  gene expression in mice disrupts the action of exendin-4 to facilitate CICR in the  $\beta$ -cells of these mice. Thus, in the present study, in which wild-type (WT) C57BL/6 mouse  $\beta$ -cells were loaded with the photolabile  $\text{Ca}^{2+}$  chelator NP-EGTA, the UV flash photolysis-catalysed uncaging of  $\text{Ca}^{2+}$  generated CICR in only 9% of the  $\beta$ -cells tested, whereas CICR was generated in 82% of the  $\beta$ -cells pretreated with exendin-4. This action of exendin-4 to facilitate CICR was reproduced by cAMP analogues that activate protein kinase A (6-Bnz-cAMP-AM) or Epac2 (8-pCPT-2'-O-Me-cAMP-AM) selectively. However, in  $\beta$ -cells of PLC- $\epsilon$  KO mice, and also Epac2 KO mice, these test substances exhibited differential efficacies in the CICR assay such that exendin-4 was partly effective, 6-Bnz-cAMP-AM was fully effective, and 8-pCPT-2'-O-Me-cAMP-AM was without significant effect. Importantly, transduction of PLC- $\epsilon$  KO  $\beta$ -cells with recombinant PLC- $\epsilon$  rescued the action of 8-pCPT-2'-O-Me-cAMP-AM to facilitate CICR, whereas a K2150E PLC- $\epsilon$  with a mutated Ras association (RA) domain, or a H1640L PLC- $\epsilon$  that is catalytically dead, were both ineffective. Since 8-pCPT-2'-O-Me-cAMP-AM failed to facilitate CICR in WT  $\beta$ -cells transduced with a GTPase activating protein (RapGAP) that downregulates Rap activity, the available evidence indicates that a signal transduction 'module' comprised of Epac2, Rap and PLC- $\epsilon$  exists in  $\beta$ -cells, and that the activities of Epac2 and PLC- $\epsilon$  are key determinants of CICR in this cell type.

(Received 25 August 2010; accepted after revision 27 October 2010; first published online 1 November 2010)

**Corresponding author** G. G. Holz: SUNY Upstate Medical University, IHP 4310 at 505 Irving Avenue, Syracuse, NY 13210, USA. Email: holzg@upstate.edu

**Abbreviations** 6-Bnz-cAMP-AM, *N*<sup>6</sup>-benzoyladenine-3',5'-cyclic monophosphate acetoxymethyl ester; 8-pCPT-2'-O-Me-cAMP-AM, 8-(4-chlorophenylthio)-2'-O-methyladenosine-3',5'-cyclic monophosphate acetoxymethyl ester; BIM-1, bisindolylmaleimide-1; CaMKII,  $\text{Ca}^{2+}$ /calmodulin-regulated protein kinase II; cAMP-GEF, cAMP-regulated guanine nucleotide exchange factor; CICR,  $\text{Ca}^{2+}$ -induced  $\text{Ca}^{2+}$  release; Epac, exchange protein directly activated by cAMP; ER, endoplasmic reticulum; ESCA-AM, Epac-selective cAMP analogue acetoxymethyl ester; EYFP, enhanced yellow fluorescent protein; GLP-1, glucagon-like peptide-1; GLP-1R, glucagon-like peptide-1 receptor; GPCR, G protein-coupled receptor; KO, knockout; NAADP, nicotinic acid adenine dinucleotide phosphate; NP-EGTA, *o*-nitrophenyl ethylene glycol tetraacetic acid; Phosphate AM3, phosphate tris (acetoxymethyl) ester; PI, phosphoinositide; PKA, protein kinase A; PKC, protein kinase C; PLC- $\epsilon$ , phospholipase C- $\epsilon$ ; Sp-8-pCPT-2'-O-Me-cAMPS, 8-(4-chlorophenylthio)-2'-O-methyladenosine-3',5'-cyclic monophosphorothioate; SES, standard extracellular saline; VDCC, voltage-dependent  $\text{Ca}^{2+}$  channels; WT, wild-type.

## Introduction

Calcium-induced  $\text{Ca}^{2+}$  release (CICR) can occur in pancreatic  $\beta$ -cells (Islam *et al.* 1992; Lemmens *et al.* 2001; Beauvois *et al.* 2004), and  $\beta$ -cell cAMP-elevating agents such as glucagon-like peptide-1 (GLP-1) or the GLP-1 receptor (GLP-1R) agonist exendin-4 mobilize an intracellular source of  $\text{Ca}^{2+}$  by facilitating CICR (Gromada *et al.* 1995; Holz *et al.* 1999; Dyachok & Gylfe, 2004). How cAMP elevating agents exert this effect is a topic of considerable interest in view of the fact that  $\text{Ca}^{2+}$  mobilized in this manner generates an increase of cytosolic  $\text{Ca}^{2+}$  concentration ( $[\text{Ca}^{2+}]_i$ ) that is an adequate stimulus for  $\beta$ -cell exocytosis (Kang *et al.* 2003; Kang & Holz, 2003; Dyachok & Gylfe, 2004). One view is that the CICR mechanism of  $\beta$ -cells is dually governed by  $\text{Ca}^{2+}$  and cAMP such that the  $\text{Ca}^{2+}$  release mechanism operates at maximal efficiency when there is a coincident rise in  $\text{Ca}^{2+}$  and cAMP levels (Kang *et al.* 2001, 2003, 2005). This is a process of second messenger coincidence detection and it involves the activation of two principal types of cAMP binding proteins found in  $\beta$ -cells; protein kinase A (PKA) and the cAMP-regulated guanine nucleotide exchange factor designated as Epac2 (de Rooij *et al.* 1998; Kawasaki *et al.* 1998). Here we have investigated the molecular basis for cAMP-dependent control of CICR in  $\beta$ -cells, and we report that a novel phospholipase C- $\epsilon$  (PLC- $\epsilon$ ; a product of the *PLCE1* gene) couples cAMP production and Epac2 activation to the facilitation of CICR. Surprisingly, this Epac2- and PLC- $\epsilon$ -dependent mechanism of  $\beta$ -cell  $\text{Ca}^{2+}$  mobilization bears a striking resemblance to the CICR mechanism that is under the control of Epac1 and PLC- $\epsilon$  in cardiomyocytes (Oestreich *et al.* 2007, 2009).

Phospholipase C- $\epsilon$  is a phosphoinositide-specific PLC, the activity of which can be stimulated by ligand binding to G protein-coupled receptors (GPCRs) and also growth factor receptors (Kelley *et al.* 2001; Lopez *et al.* 2001; Song *et al.* 2001, 2002). For growth factor receptors, the activation of PLC- $\epsilon$  is mediated by Ras superfamily monomeric GTPases, whereas a subset of GPCRs can signal through heterotrimeric GTPases to activate PLC- $\epsilon$  (Kelley *et al.* 2004; Citro *et al.* 2007). Interestingly, studies of HEK-293 cells expressing  $\beta_2$ -adrenergic GPCRs first demonstrated an ability of adrenaline to activate PLC- $\epsilon$ , and that this effect of adrenaline was both cAMP and Epac1 mediated (Schmidt *et al.* 2001). It was proposed that the cAMP-bound form of Epac1 signals through Rap GTPase to stimulate the activity of PLC- $\epsilon$ , and that this functional coupling is explained by the binding of Rap to a Rap association (RA) domain located within PLC- $\epsilon$ . Subsequently, this novel cAMP signalling mechanism was shown to mediate  $\beta_1$ -adrenergic receptor regulation of CICR in adult mouse ventricular myocytes, thereby demonstrating a true physiological role for this pathway

(Oestreich *et al.* 2007, 2009). Since Epac2 is expressed in  $\beta$ -cells (Ozaki *et al.* 2000), and since Rap1 transduces stimulatory effects of cAMP on insulin secretion (Shibasaki *et al.* 2007), an attractive hypothesis is that cAMP-elevating agents facilitate CICR, and possibly exocytosis, by virtue of their ability to stimulate PLC- $\epsilon$  activity, and that these actions of cAMP-elevating agents are mediated by Epac2 and Rap1.

We now provide the first evidence that PLC- $\epsilon$  is expressed in mouse and human islets of Langerhans. Using an assay for CICR that involves UV flash photolysis to uncage  $\text{Ca}^{2+}$  from o-nitrophenyl ethylene glycol tetraacetic acid (NP-EGTA), we also demonstrate that the Epac2-dependent action of GLP-1R agonist exendin-4 to facilitate CICR is lost in  $\beta$ -cells isolated from mice in which there is a knockout (KO) of Epac2, and also in mice in which there is a KO of PLC- $\epsilon$ . Furthermore, selective activation of Epac2 with 8-(4-chlorophenylthio)-2'-O-methyladenosine-3',5'-cyclic monophosphate acetoxymethyl ester (8-pCPT-2'-O-Me-cAMP-AM) facilitates CICR in wild-type (WT) mouse  $\beta$ -cells, but not in  $\beta$ -cells of Epac2 and PLC- $\epsilon$  KO mice. Since this action of 8-pCPT-2'-O-Me-cAMP-AM is entirely absent in  $\beta$ -cells of WT mice overexpressing a Rap GTPase activating protein (RapGAP) that downregulates the activity of Rap, it is concluded that a signal transduction 'module' comprised of Epac2, Rap and PLC- $\epsilon$  exists in  $\beta$ -cells, and that the activities of Epac2 as well as PLC- $\epsilon$  are key determinants of CICR in this cell type.

## Methods

### Ethical approval

All experimental procedures reported here were in accordance with the ethical policy of *The Journal of Physiology* (Drummond, 2009) and were also in accordance with SUNY Upstate Medical University policies governing the ethical use of mice for experimentation (IACUC protocol no. 074). For studies involving the use of donor human islets, the islets were provided by the Islet Distribution Program (IIDP) funded by the NIH. These human islets were obtained from cadaver donors under conditions of informed consent, and appropriate safeguards were maintained for donor anonymity. Approval for the use of human islets was granted by the Institutional Review Board of SUNY Upstate Medical University.

### Generation of PLC- $\epsilon$ knockout mice

Phospholipase C- $\epsilon$  KO mice with global disruption of *PLCE1* gene expression (NCBI GeneID 74055) do not express either the long or the short form of PLC- $\epsilon$ . These PLC- $\epsilon$  KO mice were generated by the methods of homologous recombination in the laboratory of A. V. Smrcka

at the University of Rochester School of Medicine (Wang *et al.* 2005). These PLC- $\epsilon$  KO mice have been used in prior studies of cardiomyocytes (Oestreich *et al.* 2007, 2009) and astrocytes (Citro *et al.* 2007). One phenotype of these mice is a cardiac contractility defect owing to a disruption of cardiomyocyte  $\beta$ -adrenergic receptor-dependent intracellular  $\text{Ca}^{2+}$  mobilization (Wang *et al.* 2005; Oestreich *et al.* 2007, 2009). For the studies described here, colonies of PLC- $\epsilon$  ( $-/-$ ) KO mice and congenic heterozygous ( $+/-$ ) or wild-type (WT;  $+/+$ ) littermate mice located at SUNY Upstate Medical University were maintained on the C57BL/6 genetic background after six rounds of backcrossing with C57BL/6 mice obtained from Charles River Laboratories International Inc. (Wilmington, MA, USA).

### Generation of Epac2 knockout mice

Epac2 KO mice with global disruption of *RAPGEF4* gene expression (NCBI GeneID 56508) were generated in the laboratory of Y. Lu of Louisiana State University School of Medicine using a gene trapping approach (Tu *et al.* 2010). The embryonic stem cell clone used to create the Epac2 KO mouse was OST450264. For the studies described here, the Epac2 KO mice and wild-type littermate mice were maintained on the 129svEv genetic background without their having been backcrossed with any other strain of mice. Additional information concerning the characterization of the Epac2 KO mice is presented in the Supplemental Material.

### Primary culture of mouse $\beta$ -cells

The indicated strains of mice were fed a standard mouse chow (Formulab Diet, catalogue no. 5008). The mice were anaesthetized by isoflurane (4% in  $\text{O}_2$ ) administered by the inhalational route and killed by cervical dislocation. This method of killing is consistent with the recommendations of the Panel on Euthanasia of the American Veterinary Medical Association, and it has received the approval of the SUNY Upstate Medical University Animal Care and Use Committee. The pancreas was removed and digested with Liberase TL Research Grade (Roche Applied Science, Indianapolis, IN, USA; catalogue no. 05-401-020-001). Batches of 150–200 islets were subjected to mild trypsinization and dispersed by trituration in a  $\text{Ca}^{2+}$ -free saline in order to generate a single-cell suspension. Single cells were allowed to adhere to glass coverslips (25CIR-1; Fisher Scientific) coated with concanavalin A (type V; Sigma-Aldrich), and these primary cultures were maintained in a humidified incubator (95% air, 5%  $\text{CO}_2$ ) at 37°C in RPMI 1640 supplemented with 10% fetal bovine serum (FBS), 100 units  $\text{ml}^{-1}$  penicillin G and 100  $\text{mg ml}^{-1}$  streptomycin. The  $\beta$ -cells were identified on the basis of

their large diameter and granular appearance, or after immunodetection of insulin (see below).

### Measurement of $[\text{Ca}^{2+}]_i$

The fura-2 loading solution consisted of a standard extracellular saline (SES) containing (mM): 138 NaCl, 5.6 KCl, 2.6  $\text{CaCl}_2$ , 1.2  $\text{MgCl}_2$ , 10 HEPES and 5.6 D-glucose, supplemented with 1  $\mu\text{M}$  fura-2 AM, 2% FBS and 0.02% Pluronic F-127 (w/v). Cells were immersed in the fura-2 loading solution for 20–30 min at 22°C, after which the solution was replaced with fresh SES. Experiments were performed at 32°C using a TE300 inverted microscope (Nikon, Melville, NY, USA) equipped with a temperature-controlled superfusion chamber (Medical Systems Corp., Greenvale, NY, USA) and a  $\times 40$  SuperFluor oil immersion objective (Nikon, NA 1.3). Microfluorimetry was performed ratiometrically at 1.0 s intervals using a dual excitation wavelength video imaging system outfitted with an intensified CCD camera (IonOptix Corp., Milton, MA, USA). A rotating mirror delivered the excitation light at 340 or 380 nm. The emitted light was measured at 510 nm, and the average of 29 frames of 340 or 380 nm excitation imaging data was used to calculate numerator and denominator values for determination of the 340/380 ratios after background subtraction. The value of  $[\text{Ca}^{2+}]_i$  was calculated according to established methods (Grynkiewicz *et al.* 1985), and the calibration was performed as described previously (Kang *et al.* 2001; Kang & Holz, 2003) using fura-2  $[\text{K}^+]_5$  salt dissolved in calibration buffers (Molecular Probes/Invitrogen Calcium Calibration Kit 1 with  $\text{Mg}^{2+}$ ). Values of  $R_{\min}$  and  $R_{\max}$  were 0.20 and 7.70.

### Ultraviolet flash photolysis for the liberation of caged $\text{Ca}^{2+}$

Methods for the uncaging of  $\text{Ca}^{2+}$  were as described in greater detail by Kang *et al.* (2005). Briefly,  $\beta$ -cells were bathed for 60 min at 23°C in SES containing cell-permeable caged  $\text{Ca}^{2+}$  (5  $\mu\text{M}$  NP-EGTA-AM; Molecular Probes/Invitrogen). The loading solution also contained 1  $\mu\text{M}$  fura-2 AM, 2% FBS and 0.02% Pluronic F-127. The uncaging of  $\text{Ca}^{2+}$  was achieved using a flash photolysis system (Model JML-C2; Rapp OptoElectronic, Hamburg, Germany). The excitation light of 80 J intensity and 600  $\mu\text{s}$  duration was filtered using a short-pass filter (cut-off 390 nm) and was delivered through a liquid light guide to individual  $\beta$ -cells by way of the microscope objective. The intensity and duration of the flash were minimized so that no measurable photo-bleaching of fura-2 was observed. The intensity of 340 and 380 nm excitation light for detection of fura-2 was also reduced so

as to be so low as to produce no measurable uncaging of  $\text{Ca}^{2+}$  (Kang *et al.* 2005).

### Statistical analysis of CICR

Population studies were performed at the single-cell level in order to determine the percentage of cells exhibiting CICR in conditions in which the cells were treated with pharmacological agents added directly to the bath or applied to individual cells via 'puffer' pipettes. At least 10 cells per coverslip were selected, one at a time in random order, to determine basal  $[\text{Ca}^{2+}]_i$  and CICR amplitude. Calcium-induced  $\text{Ca}^{2+}$  release in mouse  $\beta$ -cells was defined as a transient increase of  $[\text{Ca}^{2+}]_i$ , the duration of which did not exceed 30 s when measured at the 10% amplitude cut-off (Fig. 1C). An additional requirement was that the increase of  $[\text{Ca}^{2+}]_i$  must have exceeded 200 nM when measured at the 50% amplitude cut-off (Fig. 1C). For these population studies, each experiment was performed in triplicate, and statistical analyses were performed using ANOVA combined with Fisher's PLSD test.

### Adenoviral transduction of $\beta$ -cells

Primary cultures of mouse  $\beta$ -cells were infected with adenovirus directing the expression of RapGAP, wild-type PLC- $\epsilon$ , a K2150E PLC- $\epsilon$  with a mutated RA2 domain that prevents Rap activation, and a H1640L PLC- $\epsilon$  that is catalytically dead. The properties of these adenoviral constructs in which there is bicistronic expression of Enhanced Yellow Fluorescent Protein (EYFP) and RapGAP or PLC- $\epsilon$  have been described previously (Oestreich *et al.* 2009). Single  $\beta$ -cells maintained on glass coverslips were incubated in serum-free culture medium containing these viruses for 2 h, after which an equivalent volume of culture medium containing 10% FBS was added for an additional overnight incubation at 37°C in a cell culture incubator. The infection medium was then replaced with a virus-free medium, and the cultures were returned to the incubator for 48 h prior to each experiment. On the day of the experiment, transduced  $\beta$ -cells were positively identified using an EYFP filter set, and measurements of  $[\text{Ca}^{2+}]_i$  were then performed using a fura-2 filter set (Kang *et al.* 2005).

### Protein kinase A activation assay

Protein kinase A activity in lysates of mouse islets was measured using a PepTag Non-Radioactive cAMP-Dependent Protein Kinase Assay kit (Promega, Madison, WI, USA). Prior to their lysis, islets were exposed to acetoxymethyl esters of PKA- or Epac-selective cAMP analogues for 30 min while equilibrated at 37°C in culture medium containing 5.6 mM glucose and gassed with 95%

air and 5%  $\text{CO}_2$ . Islets were homogenized in a PKA extraction buffer, after which the crude homogenate was subjected to centrifugation (14,000g) for 5 min at 4°C. The supernatant fraction was collected and assayed for PKA activity by addition of a PepTag A1 Peptide that is a fluorescent Kemptide [LRRASLG]. The phosphorylated form of PepTag A1 Peptide was resolved by electrophoresis on a 0.8% agarose gel (100 V, 15 min) and quantified using a ChemiDoc XRS and Quantity One image analysis software (Bio-Rad, Hercules, CA, USA).

### Western blot detection of PLC- $\epsilon$

The methods for immunoprecipitation and immunoblot detection of PLC- $\epsilon$  were as described previously (Wang *et al.* 2005) except that lysates of mouse islets or donor human islets were used as the starting material. Phospholipase C- $\epsilon$  was immunoprecipitated using a 1:500 dilution of a rabbit polyclonal antiserum (2933) that recognizes the RA2 domain of PLC- $\epsilon$ . After resolution of the immunoprecipitated proteins by SDS-PAGE, immunodetection of PLC- $\epsilon$  was performed using a 1:6000 dilution of a rabbit polyclonal antiserum (2163) that recognizes the RA1 domain of PLC- $\epsilon$ . The secondary antiserum was a 1:10 000 dilution of a goat anti-rabbit IRDye 800CW (LI-COR Bioscience, Lincoln, NE, USA). Immunoreactivity was detected using a LI-COR Odyssey Infrared Imager.

### Immunodetection of Epac2 in mouse $\beta$ -cells and rat INS-1 cells

Immunofluorescence microscopy was performed using an anti-Epac2 rabbit polyclonal antiserum (Ab1536; 1:100 dilution) as the primary antiserum. The characteristics of this antiserum are described in the Supplemental Material. Mouse  $\beta$ -cells and rat INS-1 cells (Wollheim, Geneva, Switzerland) were fixed in PBS containing 4% paraformaldehyde, and the cells were then permeabilized using 0.2% Triton X-100 dissolved in PBS. The blocking solution contained 5% goat serum and 1% bovine serum albumin in PBS. A 1:1000 dilution of goat anti-rabbit IgG antiserum conjugated to Alexa Fluor 488 (Molecular Probes/Invitrogen, catalogue no. A-11034) served as the secondary antiserum. For detection of insulin immunoreactivity, the primary antiserum was a 1:1000 dilution of a guinea-pig anti-insulin antiserum (Sigma-Aldrich, catalogue no. I-8510), and a 1:1000 dilution of goat anti-guinea-pig IgG antiserum conjugated to Alexa Fluor 594 (Molecular Probes/Invitrogen, catalogue no. A-11076) served as the secondary antiserum. For INS-1 cells, immunofluorescence corresponding to Epac2 was visualized by standard fluorescence light microscopy, and the images were captured for digitization using a  $\times 20$  objective and an EMCCD camera (Cascade 512b;

Photometrics, Tucson, AZ, USA) mounted on a Nikon TE300 inverted microscope. For mouse  $\beta$ -cells, Epac2 and insulin immunoreactivity was imaged using a LSM510 laser-scanning confocal microscope, a  $\times 100$  objective and AxioVision Software (Carl Zeiss, Inc.).

### Quantitative PCR for detection of Epac2, PLC- $\epsilon$ and GLP-1 receptor mRNA

Reverse transcriptase–quantitative polymerase chain reactions (RT-QPCRs) were performed using QuantiTect Sybr-green one-step kits (Qiagen, Valencia, CA, USA) with approximately 110 ng of template RNA. Reactions were performed using an MJ MiniOpticon cycler with 35 cycles of 94°C for 15 s, 60°C for 30 s and 72°C for 30 s, followed by a melting curve analysis from 60°C to 94°C. Products were then run on 2% agarose gels, products were gel extracted using QIAquick kits (Qiagen), and product identity was confirmed by sequencing. Threshold crossing ( $C_t$ ) values were set manually, and the differences between the  $C_t$  values were calculated for each reaction. The  $\Delta C_t$  values were entered into Origin 8 software (OriginLab, Northampton, MA, USA) for analysis using ANOVA. The PCR primers used to amplify PLC- $\epsilon$  were forward, 5'-CCTGCCCATGGACTACCTCTG-3' and reverse, 5'-GGCCACATGCACCAAATAAGA-3'. For the GLP-1R, the PCR primers were forward, 5'-CACACTGCTGGCCTTCTCGG-3' and reverse, 5'-GCAGCCCTCGTCCATAGAG-3', and for Epac2 the PCR primers were forward, 5'-CGCCATGCAACCATCGTTACC-3' and reverse, 5'-GAGCCCGTTTCCATAACACC-3'. An S18 primer set was used to generate a reference PCR product, and the relative abundance of the PCR products was calculated using the  $\Delta\Delta C_t$  method (Litvak & Schmittgen, 2001).

### Sources of reagents and administration of test substances

Phosphate-AM<sub>3</sub> (Phosphate tris (acetoxymethyl) ester), N<sup>6</sup>-benzoyladenine-3',5'-cyclic monophosphate acetoxymethyl ester (6-Bnz-cAMP-AM) and 8-pCPT-2'-O-Me-cAMP-AM were from Biolog Life Science Institute (Bremen, Germany). Exendin-4, H-89, thapsigargin and bafilomycin were from Sigma-Aldrich. Ro-31-8220, BIM-1, KN-92 and KN-93 were from Calbiochem. Each test substance was dissolved in SES and, except for H-89, which was bath applied, all test substances were applied to individual cells using glass 'puffer' micropipettes (World Precision Instruments, catalogue no. 1B150-6) under the control of a Narishige Instruments MM-203 hydraulic micromanipulator and pressurized with a pneumatic pressure ejection system, as described previously (Holz *et al.* 1993).

## Results

### Calcium-induced Ca<sup>2+</sup> release is facilitated by exendin-4 and is disrupted in $\beta$ -cells of PLC- $\epsilon$ KO mice

Wild-type (WT) 16- to 28-week-old male mice were used in combination with established methods of UV flash photolysis in order to uncage Ca<sup>2+</sup> in NP-EGTA- and fura-2-loaded  $\beta$ -cells equilibrated in SES containing 5.6 mM glucose (Kang *et al.* 2005). In this single-cell assay, a short-duration (600  $\mu$ s) flash of low-intensity UV light was delivered to a  $\beta$ -cell through the microscope objective while also monitoring the [Ca<sup>2+</sup>]<sub>i</sub>. By uncaging Ca<sup>2+</sup> in this manner, it was possible to generate a small (<50 nM) increase of [Ca<sup>2+</sup>]<sub>i</sub> that did not generate CICR on its own, either in control conditions (first UV flash of Fig. 1A) or when the uncaging of Ca<sup>2+</sup> was paired with the application of a small bolus of SES to the cell (second UV flash of Fig. 1A). However, if the uncaging of Ca<sup>2+</sup> was performed while also administering exendin-4 (10 nM), a large transient increase of [Ca<sup>2+</sup>]<sub>i</sub> was generated (Fig. 1B). As reported for mouse  $\beta$ -cells previously, this action of exendin-4 was explained by its ability to sensitize the intracellular Ca<sup>2+</sup> release mechanism to stimulatory effects of cytosolic Ca<sup>2+</sup>, thereby allowing CICR to be triggered by the uncaging of Ca<sup>2+</sup> (Kang *et al.* 2005). Note that in these conditions of NP-EGTA loading, exendin-4 failed to stimulate an increase of [Ca<sup>2+</sup>]<sub>i</sub> prior to the uncaging of Ca<sup>2+</sup> (Fig. 1B). This finding is consistent with our previous study of mouse  $\beta$ -cells, in which we demonstrated that in conditions of NP-EGTA loading, exendin-4 does not depolarize  $\beta$ -cells (Kang *et al.* 2005). Thus, the UV flash photolysis assay described here allows a selective analysis of the CICR mechanism independent of any confounding depolarizing action of exendin-4 that would stimulate Ca<sup>2+</sup> influx through voltage-dependent Ca<sup>2+</sup> channels (VDCCs).

We defined the appearance of CICR as a transient increase of [Ca<sup>2+</sup>]<sub>i</sub>, the duration of which did not exceed 30 s when measured at the 10% amplitude cut-off (Fig. 1C). An additional requirement was that the increase of [Ca<sup>2+</sup>]<sub>i</sub> must have exceeded 200 nM when measured at the 50% amplitude cut-off (Fig. 1C). Using these criteria, population studies were conducted at the single-cell level using  $\beta$ -cells of WT mice. It was found that CICR could be generated in 9% of the  $\beta$ -cells not exposed to exendin-4, whereas 82% of the cells exhibited CICR when they were pretreated with exendin-4 (10 nM; Fig. 1D). When the PKA inhibitor H-89 (10  $\mu$ M) was included in the SES bathing these exendin-4-treated cells, the percentage of responsive cells decreased from 82 to 55% (Fig. 1D), thereby demonstrating that exendin-4 acted through PKA-dependent and PKA-independent pathways to facilitate CICR.

This analysis was then repeated using 16- to 28-week-old male PLC- $\epsilon$  KO mice that were congenic

with the WT mice described above. In comparison to findings obtained with WT mouse  $\beta$ -cells, the percentage of exendin-4-treated  $\beta$ -cells exhibiting CICR was reduced for PLC- $\epsilon$  KO mouse  $\beta$ -cells not treated with H-89. Thus, 82% of the exendin-4-treated  $\beta$ -cells from WT mice exhibited CICR, whereas only 44% of the  $\beta$ -cells of PLC- $\epsilon$  KO mice exhibited CICR (Fig. 1D). Furthermore, in conditions of H-89 treatment, the action of exendin-4 in PLC- $\epsilon$  KO mouse  $\beta$ -cells was nearly abrogated (Fig. 1D). In summary, in WT mouse  $\beta$ -cells, exendin-4 was found to facilitate CICR in a manner that was both PKA and PLC- $\epsilon$  dependent.

### Calcium-induced $\text{Ca}^{2+}$ release is facilitated by the acetoxymethyl esters of PKA- and Epac-selective cAMP analogues

Additional studies were performed using cAMP analogues that activate PKA (6-Bnz-cAMP-AM) or Epac (8-pCPT-2'-O-Me-cAMP-AM) in a selective manner.

Such compounds are membrane-permeant acetoxymethyl esters that must be hydrolysed by cytosolic esterases in order to become bioactive (Vliem *et al.* 2008; Chepurny *et al.* 2009). To assess the efficacy of these compounds, it was first established that CICR in WT mouse  $\beta$ -cells was not facilitated by phosphate-AM<sub>3</sub> (0.3  $\mu\text{M}$ ; Fig. 2A). This unsubstituted acetoxymethyl ester serves as a negative control because it does not activate cAMP binding proteins, but it does generate 3 mole equivalents of acetic acid and formaldehyde per mole of phosphate when it is hydrolysed by cytosolic esterases. Having established this negative control, it was then demonstrated that CICR was instead facilitated by PKA-selective 6-Bnz-cAMP-AM (Fig. 2B) and also Epac-selective 8-pCPT-2'-O-Me-cAMP-AM (Fig. 2C; abbreviated as ESCA-AM) when each analogue was tested at a concentration of 1  $\mu\text{M}$ . For 8-pCPT-2'-O-Me-cAMP-AM, this facilitation was not explained by its unexpected ability to activate PKA, as verified in an *in vitro* PKA activation assay using isolated mouse islets treated with

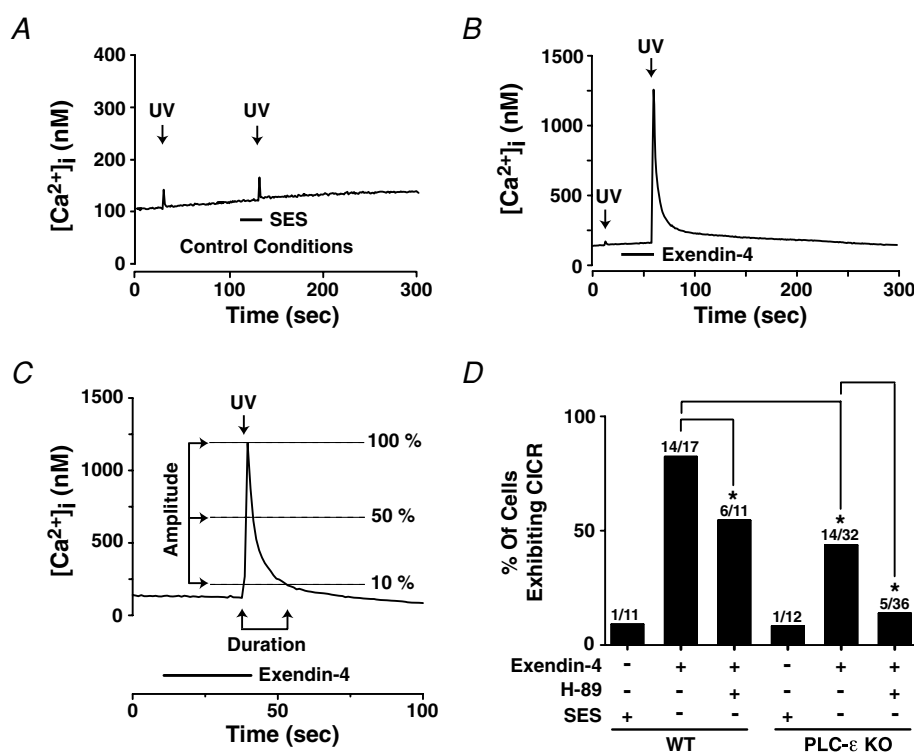


**Figure 1. Calcium-induced  $\text{Ca}^{2+}$  release (CICR) facilitated by exendin-4 is disrupted in  $\beta$ -cells of phospholipase C- $\epsilon$  (PLC- $\epsilon$ ) knockout (KO) mice**

A, CICR was not observed in control conditions in which the uncaging of  $\text{Ca}^{2+}$  (UV, arrows) was paired with the application of standard extracellular saline (SES; horizontal bar) to a wild-type (WT) mouse  $\beta$ -cell. B, CICR was observed when exendin-4 (10 nM) was applied to a WT mouse  $\beta$ -cell while also uncaging  $\text{Ca}^{2+}$  (note different y-axis scaling in A and B). C, CICR amplitude was determined by subtracting the baseline  $[\text{Ca}^{2+}]_i$  from the  $[\text{Ca}^{2+}]_i$  measured at the peak of the  $\text{Ca}^{2+}$  transient. Values of  $[\text{Ca}^{2+}]_i$  corresponding to 10 and 50% of the peak  $[\text{Ca}^{2+}]_i$  were then determined in order to calculate the percentage of cells exhibiting CICR. D, population studies of  $\beta$ -cells from WT or PLC- $\epsilon$  KO mice examining the action of exendin-4 (10 nM) to facilitate CICR. Fractions above the histogram bars indicate the number of cells exhibiting CICR (numerator) and the number of cells tested (denominator), here and in subsequent figures. \* $P < 0.01$ . H-89 was tested at 10  $\mu\text{M}$ .

this analogue (Supplemental Material, Fig. S1A). Thus, it was not surprising that the action of 6-Bnz-cAMP-AM to facilitate CICR was blocked by H-89 (10  $\mu$ M), whereas the action of 8-pCPT-2'-O-Me-cAMP-AM was not (compare insets of Fig. 2B and C; also refer to the statistics concerning this experiment that are presented in Fig. 3E and F).

**Calcium-induced  $\text{Ca}^{2+}$  release is facilitated by a hydrolysis-resistant Sp-8-pCPT-2'-O-Me-cAMPS**

It has recently become appreciated that the non-acetoxymethyl ester 8-pCPT-2'-O-Me-cAMP is metabolized intracellularly via hydrolysis to generate bioactive derivatives of adenosine, and that such

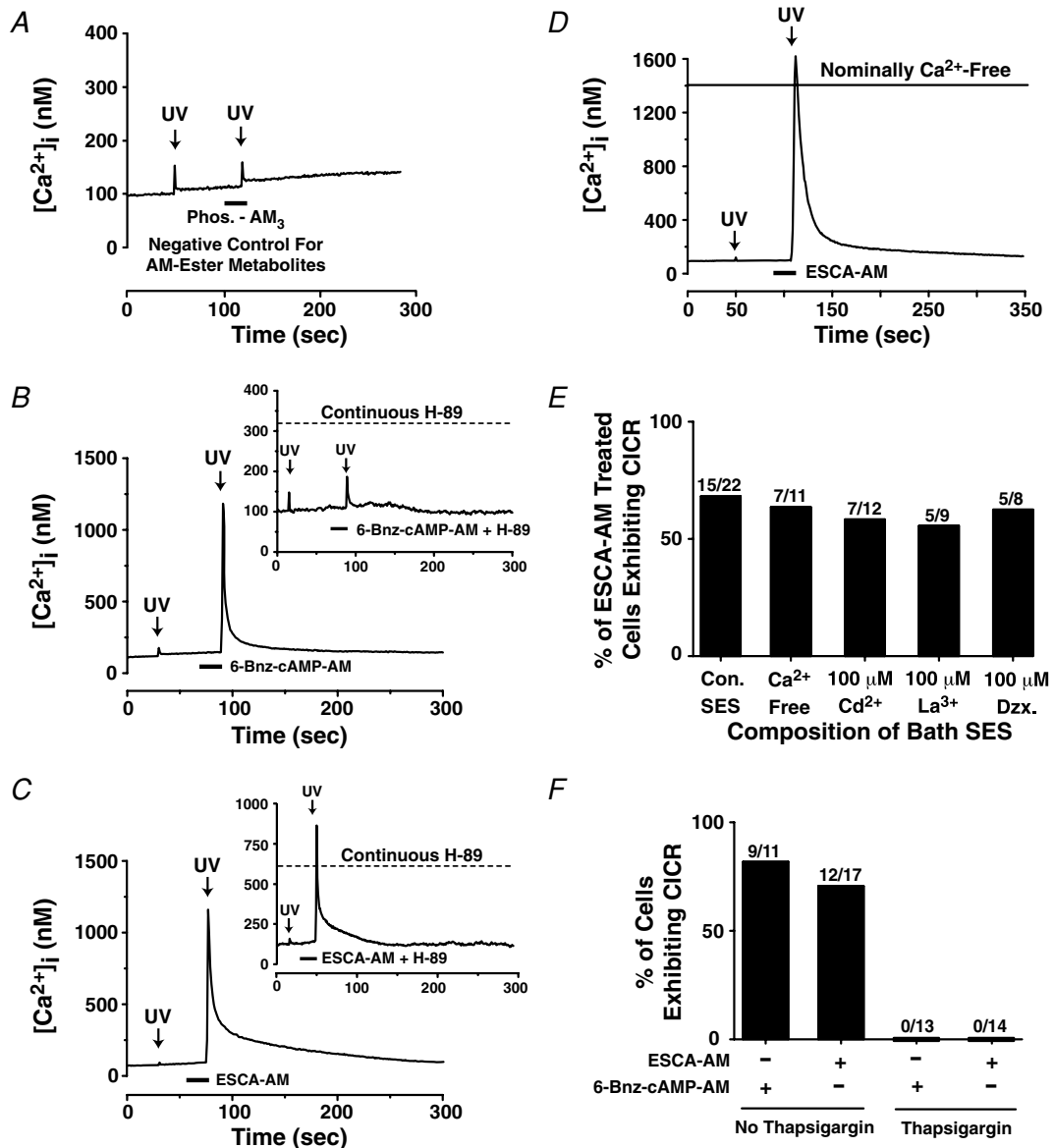


**Figure 2. Protein kinase A (PKA)-dependent and PKA-independent regulation of CICR in mouse  $\beta$ -cells**  
 A, in conditions of UV flash photolysis, CICR was not facilitated by phosphate-AM<sub>3</sub> (Phos.-AM<sub>3</sub>; 0.3  $\mu$ M) in a WT mouse  $\beta$ -cell bathed in SES containing  $\text{Ca}^{2+}$ . B, 6-Bnz-cAMP-AM (1  $\mu$ M) facilitated CICR in a WT mouse  $\beta$ -cell, an effect blocked by H-89 (10  $\mu$ M, inset). C, 8-pCPT-2'-O-Me-cAMP-AM (1  $\mu$ M; ESCA-AM) facilitated CICR in a WT mouse  $\beta$ -cell, an effect not blocked by H-89 (10  $\mu$ M, inset). D and E, CICR facilitated by 8-pCPT-2'-O-Me-cAMP-AM (1  $\mu$ M) was measurable in conditions in which WT mouse  $\beta$ -cells were bathed in SES that was nominally  $\text{Ca}^{2+}$  free (D) or that contained  $\text{Ca}^{2+}$  supplemented with diazoxide (Dzx.),  $\text{Cd}^{2+}$  or  $\text{La}^{2+}$  (E). F, neither 8-pCPT-2'-O-Me-cAMP-AM (1  $\mu$ M) nor 6-Bnz-cAMP-AM (1  $\mu$ M) retained an ability to facilitate CICR in WT mouse  $\beta$ -cells treated with thapsigargin (1  $\mu$ M).

derivatives can affect cellular functions in an Epac-independent manner (Laxman *et al.* 2006). This phenomenon is especially apparent after prolonged exposure (48–96 h) of cells to 8-pCPT-2'-O-Me-cAMP (Enyeart *et al.* 2010). Importantly, such a confounding metabolic process does not explain the rapid action of 8-pCPT-2'-O-Me-cAMP-AM to facilitate CICR, as reported here. In fact, we found that CICR was facilitated by the Epac activator Sp-8-pCPT-2'-O-Me-cAMPS, a hydrolysis-resistant cAMP analogue that is not metabolized to bioactive derivatives of adenosine (Supplemental Material, Fig. S1B). Given that Sp-8-pCPT-2'-O-Me-cAMPS is not an acetoxymethyl ester, it exerted an expected reduced efficacy in this

assay (Supplemental Material, Fig. S1B). Increasing the concentration of Sp-8-pCPT-2'-O-Me-cAMPS from 1 to 100  $\mu\text{M}$  led to a significant increase in the fraction of cells exhibiting CICR ( $P < 0.05$ ).

### Calcium-induced $\text{Ca}^{2+}$ release is generated by the release of $\text{Ca}^{2+}$ from thapsigargin-sensitive $\text{Ca}^{2+}$ stores

The transient increase of  $[\text{Ca}^{2+}]_i$  that was generated in response to the uncaging of  $\text{Ca}^{2+}$  in WT mouse  $\beta$ -cells treated with 8-pCPT-2'-O-Me-cAMP-AM signified the mobilization of intracellular  $\text{Ca}^{2+}$  due to the fact that it could still be measured in conditions in which

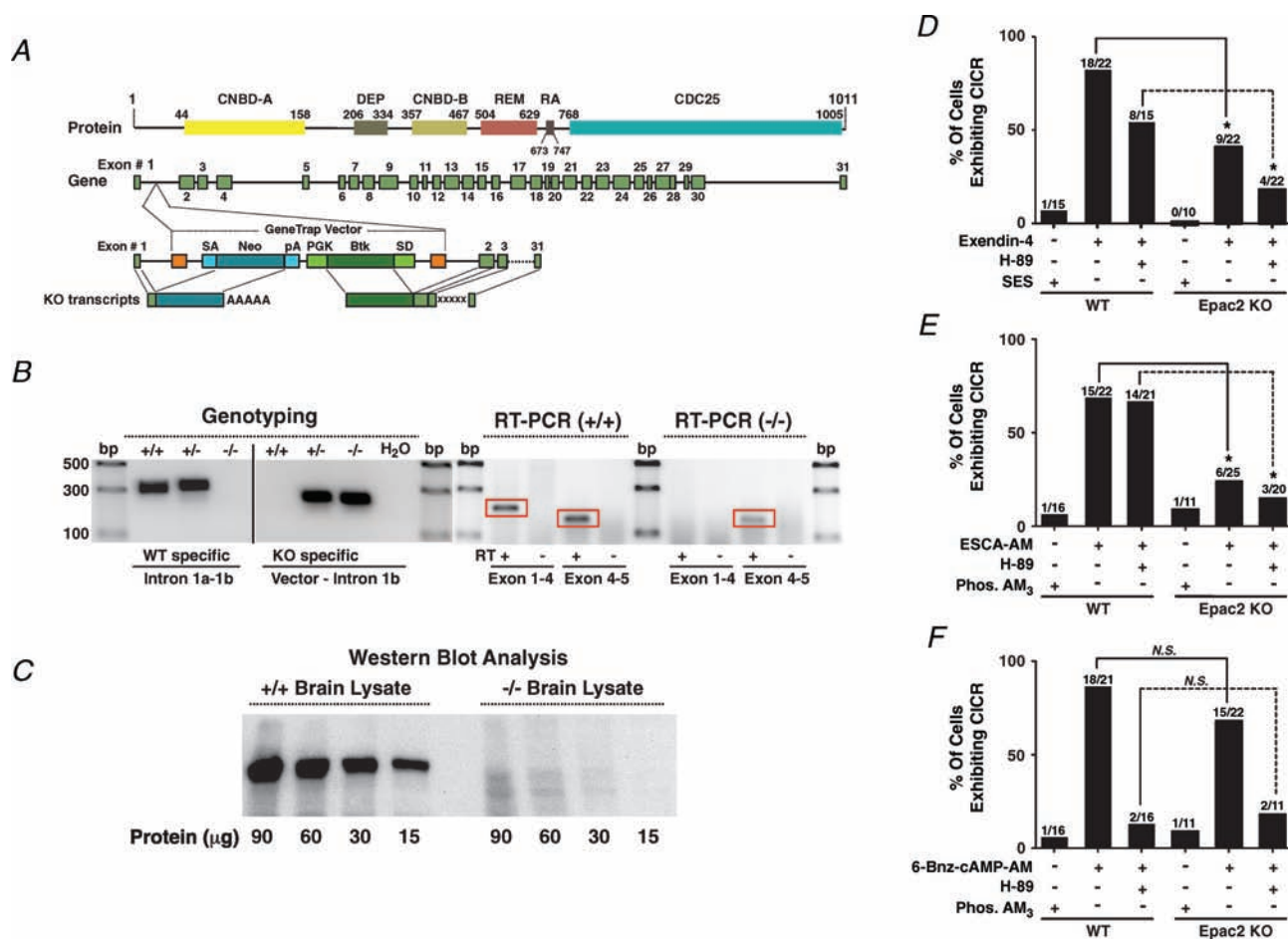


**Figure 3. Calcium-induced  $\text{Ca}^{2+}$  release facilitated by exendin-4 is disrupted in  $\beta$ -cells of Epac2 KO mice**  
**A**, domain structure of Epac2 (top), gene structure of *RAGGEF4* (middle) and construction of the gene trap targeting vector (bottom) used to generate the KO of Epac2. **B**, confirmation of the KO by genotyping (left) and by RT-PCR (right). **C**, confirmation of the KO by Western blot using monoclonal antibody (5B1) and lysates of mouse brain. See Supplemental Material for additional details. **D–F**, illustrated are the percentages of WT or Epac2 KO mouse  $\beta$ -cells exhibiting CICR in conditions of exendin-4 (10 nM), 8-pCPT-2'-O-Me-cAMP-AM (1  $\mu\text{M}$ ) or 6-Bnz-cAMP-AM (1  $\mu\text{M}$ ) treatment with or without H-89 (10  $\mu\text{M}$ ). The KO of Epac2 diminished the action of exendin-4 (**D**) and strongly suppressed the action of 8-pCPT-2'-O-Me-cAMP-AM (**E**) to facilitate CICR. However, 6-Bnz-cAMP-AM retained its ability to facilitate CICR in  $\beta$ -cells of Epac2 KO mice, and this action of 6-Bnz-cAMP-AM was nearly abrogated by treatment with H-89 (**F**). Note that the H-89-resistant action of 8-pCPT-2'-O-Me-cAMP-AM was missing in  $\beta$ -cells of Epac2 KO mice (**E**).

$\beta$ -cells were bathed in SES that was nominally  $\text{Ca}^{2+}$  free, or that was supplemented with agents that blocked  $\text{Ca}^{2+}$  influx, such as  $\text{Cd}^{2+}$ ,  $\text{La}^{3+}$  or diazoxide (Fig. 2D and E). In contrast, the transient increase of  $[\text{Ca}^{2+}]_i$  was not generated in conditions in which the endoplasmic reticulum (ER)  $\text{Ca}^{2+}$  content was depleted by treatment with sarcoplasmic–endoplasmic  $\text{Ca}^{2+}$ -ATPase inhibitor thapsigargin ( $1\ \mu\text{M}$ ; Fig. 2F; Supplemental Material, Fig. S2A). Such findings are expected if 8-pCPT-2'-O-Me-cAMP-AM mobilizes  $\text{Ca}^{2+}$  from ER  $\text{Ca}^{2+}$  stores (Kang *et al.* 2005). These ER  $\text{Ca}^{2+}$  stores may also be mobilized in a PKA-dependent manner, since thapsigargin treatment also abrogated the action of 6-Bnz-cAMP-AM to release intracellular  $\text{Ca}^{2+}$  (Fig. 2F; Supplemental Material, Fig. S2B).

Since recent reports indicate that Epac activators might signal through  $\beta$ -cell nicotinic acid adenine dinucleotide phosphate (NAADP) receptors (i.e. two-pore  $\text{Ca}^{2+}$  channels) to mobilize  $\text{Ca}^{2+}$  from 'acidic  $\text{Ca}^{2+}$  stores' located in a non-ER compartment (Kim *et al.* 2008; Naylor *et al.* 2009), we also tested the vacuolar

$\text{H}^+$  ATPase inhibitor bafilomycin A1. This compound disrupts the mobilization of  $\text{Ca}^{2+}$  from acidic  $\text{Ca}^{2+}$  stores that are under the control of NAADP (Calcraft *et al.* 2009). When WT mouse  $\beta$ -cells were treated with bafilomycin A1 ( $1\ \mu\text{M}$ ), a gradual increase of the basal  $[\text{Ca}^{2+}]_i$  was measured, and from this new plateau it was still possible to evoke CICR in conditions of UV flash photolysis provided that the cells were also treated with 8-pCPT-2'-O-Me-cAMP-AM (Supplemental Material, Fig. S2C–F). Thus, the facilitatory action of 8-pCPT-2'-O-Me-cAMP-AM measured in this assay of CICR might not be related to the release of  $\text{Ca}^{2+}$  from acidic  $\text{Ca}^{2+}$  stores, although this possibility remains to be explored in greater detail.

#### Assessment of CICR in $\beta$ -cells of Epac2 KO mice

Since no suitable pharmacological antagonist of Epac2 activation exists (Holz *et al.* 2008), we used global Epac2 KO mice in order to definitively establish a role for Epac2 in the facilitation of CICR by Epac activators.

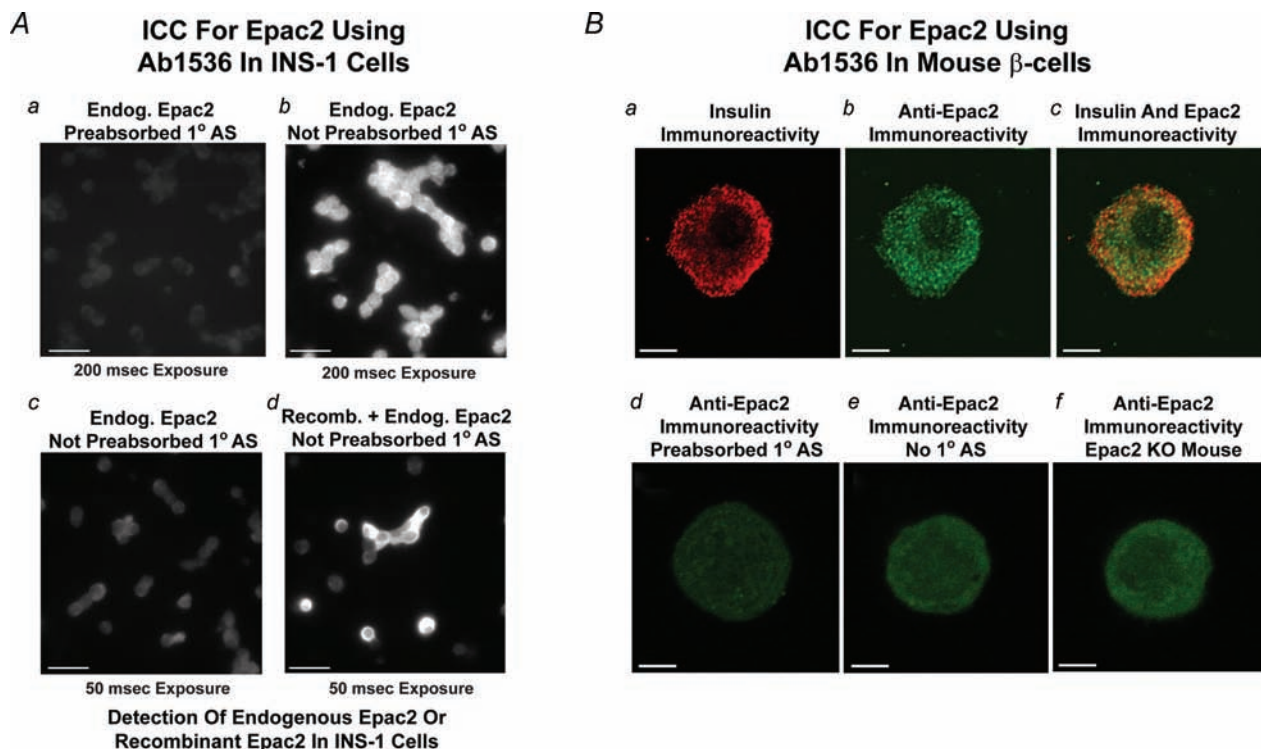


**Figure 4. Rabbit polyclonal Ab1536 recognizes Epac2 in INS-1 cells and mouse  $\beta$ -cells**

Aa and b, immunofluorescence cytochemistry (ICC) demonstrated that Epac2 in INS-1 cells was not detected using Ab1536 preabsorbed with a peptide that was used for immunization and antibody production (Aa), whereas Epac2 was detected using Ab1536 that was not preabsorbed (Ab). Ac and d, overexpression of recombinant mouse Epac2 in INS-1 cells increased Epac2 immunoreactivity when comparing the signal obtained with mock transfected cells (Ac) or transfected cells (Ad). Ba–c, co-detection of insulin and Epac2 in a mouse  $\beta$ -cell. Bd–f, control cells demonstrating that Epac2 immunoreactivity was not detected when the primary antiserum ( $1^\circ$  AS) was preabsorbed with the immunogen peptide (Bd), or when no primary antiserum was included in the processing buffer (Be), or when ICC was performed using both the primary and secondary antisera and an Epac2 KO mouse  $\beta$ -cell (Bf). Calibration bars for A and B represent 10 and  $3.5\ \mu\text{m}$ , respectively.

These Epac2 KO mice were generated using a gene trap approach that inserted into intron 1 of *RAPGEF4* a transgene incorporating multiple translation stop codons in multiple reading frames (Fig. 3A). The KO of Epac2 in these mice was confirmed by methods of genotyping and RT-PCR (Fig. 3B) and by Western blot analysis using a monoclonal (5B1) anti-Epac2 antibody (Fig. 3C). Importantly, expression of Epac2 was confirmed in the  $\beta$ -cells of WT mice, as detected by immunofluorescence microscopy using a rabbit affinity-purified anti-Epac2 antiserum (Ab1536). This antiserum also recognizes endogenous and recombinant forms of Epac2 in rat INS-1 cells (Fig. 4A and B). Furthermore, Epac2 was also detected in donor human islets, a finding not previously documented using anti-Epac2 antisera (Supplemental Material, Fig. S3).

Using  $\beta$ -cells of Epac2 KO mice, it was demonstrated that the action of exendin-4 (10 nM) to facilitate CICR was reduced but not abrogated relative to the action

of exendin-4 in WT mouse  $\beta$ -cells (Fig. 3D). This analysis also demonstrated that in  $\beta$ -cells of WT mice, the action of exendin-4 was only partly inhibited by H-89 (10  $\mu$ M), and that the H-89-resistant action of exendin-4 was reduced in  $\beta$ -cells of Epac2 KO mice (Fig. 3D). Importantly, this analysis also revealed that the action of 8-pCPT-2'-O-Me-cAMP-AM to facilitate CICR was strongly suppressed in  $\beta$ -cells of Epac2 KO mice, as measured in conditions in which  $\beta$ -cells were not treated, or treated, with H-89 (Fig. 3E). In contrast, 6-Bnz-cAMP-AM retained its ability to facilitate CICR in  $\beta$ -cells of Epac2 KO mice not treated with H-89, whereas little or no action of 6-Bnz-cAMP-AM was measurable after treatment of these  $\beta$ -cells with H-89 (Fig. 3F). In summary, in conditions in which Epac2 expression was ablated, the  $\text{Ca}^{2+}$  mobilizing action of exendin-4 was diminished, the action of 8-pCPT-2'-O-Me-cAMP-AM was abrogated, and the action of 6-Bnz-cAMP-AM was unaffected.

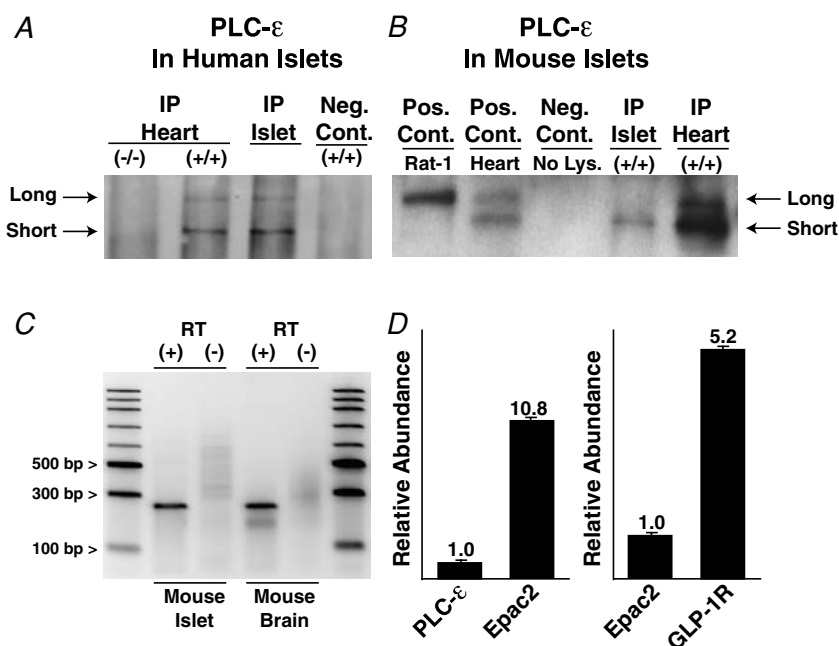


**Figure 5. Phospholipase C- $\epsilon$  is expressed in mouse and human islets**

A, illustrates an immunoblot obtained using lysates of either human islets or mouse hearts from WT mice (+/+) or PLC- $\epsilon$  KO mice (-/-). Phospholipase C- $\epsilon$  in these lysates was immunoprecipitated (IP) and resolved by SDS-PAGE for immunodetection. The negative control (Neg. Cont.) was a mock IP of WT mouse heart lysate to which no antiserum was added. B, immunodetection of PLC- $\epsilon$  was performed using lysates of WT mouse islets and heart, and also Rat-1 fibroblasts. Positive controls (Pos. Cont.) were lysates not subjected to immunoprecipitation. The negative control refers to the absence of added lysate (Lys.). Note that in both human and mouse islets, the short form (ca 200 kDa) of PLC- $\epsilon$  is expressed at levels higher than that of the longer form (ca 250 kDa). C, RT-PCR for PLC- $\epsilon$  mRNA expression in male C57BL/6 mouse islets and brain using a primer set that amplifies residues 1703–1927 of Reference Sequence NM\_019588.2. D, RT-QPCR analysis of the relative levels of expression of PLC- $\epsilon$ , Epac2 and GLP-1R mRNAs in male C57BL/6 mouse islets using the PLC- $\epsilon$  primer set listed for C and additional primer sets that amplify residues 367–506 of Epac2 (NM\_019688) and residues 816–948 of the GLP-1R (NM\_002062.3). Error bars indicate standard deviations for two experiments.

**8-pCPT-2'-O-Me-cAMP-AM fails to facilitate CICR in  $\beta$ -cells of PLC- $\epsilon$  KO mice**

Phospholipase C- $\epsilon$  was detectable by Western blot analysis (Fig. 5A and B) and by PCR analysis (Fig. 5C and D) using mouse islets and also donor human islets. Thus, attention turned to evaluating the functional consequences of the PLC- $\epsilon$  KO when testing PKA- and Epac-selective cAMP analogues. Using an approach identical to that described for Epac2 KO mice, it was demonstrated that 6-Bnz-cAMP-AM retained its efficacy to facilitate CICR in  $\beta$ -cells of PLC- $\epsilon$  KO mice (Fig. 6A), whereas 8-pCPT-2'-O-Me-cAMP-AM was ineffective (Fig. 6B). This reduced efficacy of 8-pCPT-2'-O-Me-cAMP-AM in  $\beta$ -cells of PLC- $\epsilon$  KO mice was unlikely to be explained by a reduction of ER Ca<sup>2+</sup> content. This fact was established by demonstrating that the amplitudes of the cytosolic Ca<sup>2+</sup>

transients measured in conditions of UV flash photolysis were nearly identical when evaluating the action of 6-Bnz-cAMP-AM (1  $\mu$ M) to facilitate CICR in  $\beta$ -cells of WT mice vs. PLC- $\epsilon$  KO mice (1,205  $\pm$  120 nM for  $n$  = 11 WT  $\beta$ -cells vs. 1,156  $\pm$  140 nM for  $n$  = 12 PLC- $\epsilon$  KO  $\beta$ -cells). As predicted, in  $\beta$ -cells of PLC- $\epsilon$  KO mice the action of 6-Bnz-cAMP-AM was fully blocked by H-89 (Fig. 6A), whereas the small and non-significant residual action of 8-pCPT-2'-O-Me-cAMP-AM was not significantly reduced by H-89 (Fig. 6B). Taken together, these findings provide strong support for a model in which there exist not only PKA- but also Epac2-mediated actions of cAMP to facilitate CICR. More importantly, these findings obtained using PLC- $\epsilon$  KO mice indicate that PLC- $\epsilon$  serves as the principal effector signalling molecule in support of CICR that is facilitated by activators of Epac2 but not PKA.

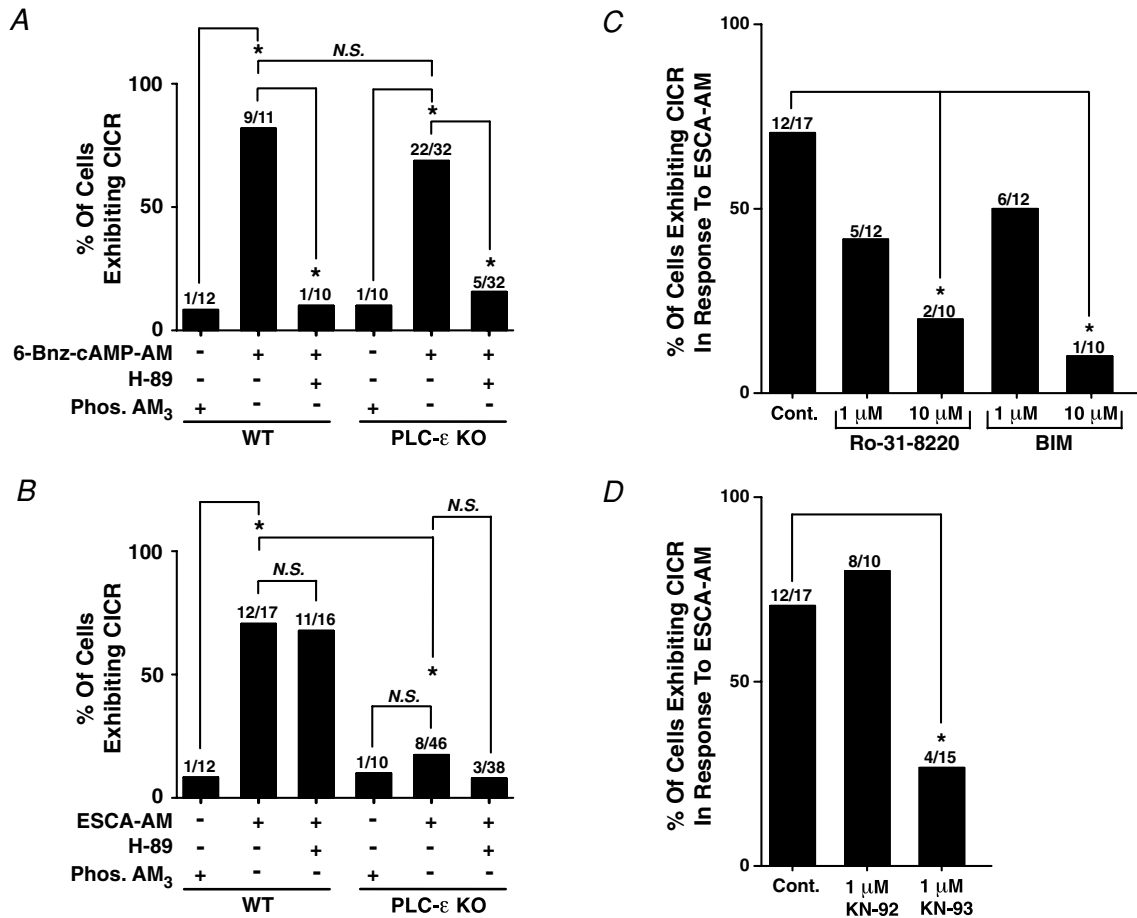


**Figure 6. Calcium-induced Ca<sup>2+</sup> release is under the control of PLC- $\epsilon$ , protein kinase C (PKC) and CaMKII**  
 A, population studies illustrating the H-89 (10  $\mu$ M)-sensitive action of 6-Bnz-cAMP-AM (1  $\mu$ M) to sensitize CICR in  $\beta$ -cells of both WT and PLC- $\epsilon$  KO mice. B, population studies illustrating the H-89-resistant action of 8-pCPT-2'-O-Me-cAMP-AM (1  $\mu$ M) to facilitate CICR in  $\beta$ -cells of WT but not PLC- $\epsilon$  KO mice. C and D, population studies illustrating the actions of PKC inhibitors Ro-31-8220 and BIM-1 (C) or the CaMKII inhibitor KN-93 but not the inert KN-92 (D) to suppress CICR facilitated by 8-pCPT-2'-O-Me-cAMP-AM (1  $\mu$ M; ESCA-AM). \* $P$  < 0.001.

## Evidence that CICR is regulated by PKC and Ca<sup>2+</sup>/calmodulin-regulated protein kinase II

Epac-selective cAMP analogues stimulate the release of Ca<sup>2+</sup> from the sarcoplasmic reticulum of adult mouse and rat ventricular cardiomyocytes (Oestreich *et al.* 2007, 2009; Pereira *et al.* 2007). Such actions of the analogues are mediated by protein kinase C- $\epsilon$  (PKC- $\epsilon$ ) and Ca<sup>2+</sup>/calmodulin-regulated protein kinase II (CaMKII) acting in their roles as downstream effectors of PLC- $\epsilon$ . In fact, the PKC- $\epsilon$ -mediated phosphorylation of CaMKII is proposed to play a key role in regulating the function of ryanodine receptor (RYR2) Ca<sup>2+</sup> release channels in adult mouse ventricular cardiomyocytes (Oestreich *et al.* 2009). Therefore, it is remarkable that in WT mouse  $\beta$ -cells, bath application of the PKC inhibitors Ro-31-8220 and BIM-1 suppressed the action of 8-pCPT-2'-O-Me-cAMP-AM to facilitate CICR (Fig. 6C). Furthermore, CICR was also suppressed by the CaMKII inhibitor KN-93, whereas KN-92 was inactive (Fig. 6D; KN-92 does not inhibit CaMKII). These effects of PKC and CaMKII inhibitors were measurable when each was tested at concentrations (1–10  $\mu$ M) that disrupt Epac1- and PLC- $\epsilon$ -regulated CICR in cardiomyocytes (Pereira *et al.* 2007; Oestreich *et al.* 2009).

## Recombinant PLC- $\epsilon$ rescues CICR in $\beta$ -cells of PLC- $\epsilon$ KO mice

The failure of 8-pCPT-2'-O-Me-cAMP-AM to facilitate CICR in  $\beta$ -cells of PLC- $\epsilon$  KO mice might simply result from the absence of PLC- $\epsilon$  in these cells. Alternatively, there might exist compensatory processes (e.g. reduced Epac2 or Rap GTPase expression; upregulation of RapGAP activity) that are initiated by the KO of PLC- $\epsilon$ , and that disrupt CICR by virtue of their abilities to alter signalling pathways that are Epac2 and Rap dependent, but that do not involve PLC- $\epsilon$ . The first of these two alternative possibilities is the more likely explanation because the facilitation of CICR by 8-pCPT-2'-O-Me-cAMP-AM could be rescued after transduction of PLC- $\epsilon$  KO  $\beta$ -cells with a bicistronic adenovirus that directed expression of WT recombinant PLC- $\epsilon$  in combination with EYFP. In this assay, EYFP served as a fluorescent marker with which to obtain a positive identification of transduced cells in conditions of imaging that still allowed accurate fura-2-based measurements of [Ca<sup>2+</sup>]<sub>i</sub> (Kang *et al.* 2005).

Using these imaging techniques, it was first demonstrated that 8-pCPT-2'-O-Me-cAMP-AM (1  $\mu$ M) failed to alter [Ca<sup>2+</sup>]<sub>i</sub> in PLC- $\epsilon$  KO mouse  $\beta$ -cells that were transduced with EYFP but not PLC- $\epsilon$ , and that were NP-EGTA loaded but not subjected to UV flash photolysis (Fig. 7A). The experiment was then repeated using PLC- $\epsilon$  KO mouse  $\beta$ -cells transduced with EYFP

and also recombinant PLC- $\epsilon$ . Remarkably, the cells expressing EYFP and recombinant PLC- $\epsilon$  were extremely sensitive to 8-pCPT-2'-O-Me-cAMP-AM (1  $\mu$ M) such that oscillations of [Ca<sup>2+</sup>]<sub>i</sub> were induced in the absence of UV flash photolysis (Fig. 7B). Although the nature of these oscillations was not investigated, such findings are understandable if high-level expression of recombinant PLC- $\epsilon$  in PLC- $\epsilon$  KO  $\beta$ -cells allows a more efficient coupling of endogenous Epac2 activation to the mobilization of intracellular Ca<sup>2+</sup>. This conclusion is supported by the finding that no such oscillations of [Ca<sup>2+</sup>]<sub>i</sub> were measured when the concentration of 8-pCPT-2'-O-Me-cAMP-AM was reduced to 0.3  $\mu$ M (Fig. 7C).

Having established that a lower concentration of 8-pCPT-2'-O-Me-cAMP-AM (0.3  $\mu$ M) failed to alter basal [Ca<sup>2+</sup>]<sub>i</sub> in PLC- $\epsilon$  KO mouse  $\beta$ -cells transduced with recombinant PLC- $\epsilon$ , it was then possible to perform a UV flash photolysis assay in which this same concentration of 8-pCPT-2'-O-Me-cAMP-AM was evaluated for its potential ability to facilitate CICR. It was demonstrated that transduction of PLC- $\epsilon$  KO mouse  $\beta$ -cells with recombinant PLC- $\epsilon$  rescued the action of 8-pCPT-2'-O-Me-cAMP-AM (0.3  $\mu$ M) to facilitate CICR initiated by the uncaging of Ca<sup>2+</sup> (Fig. 7D and F). However, no such rescue occurred when PLC- $\epsilon$  KO  $\beta$ -cells were transduced with EYFP alone (Fig. 7E and F). It may be concluded that the absence of PLC- $\epsilon$  expression does in fact explain the loss-of-function phenotype in which activators of Epac2 failed to facilitate CICR in the  $\beta$ -cells of PLC- $\epsilon$  KO mice.

## Facilitation of CICR by 8-pCPT-2'-O-Me-cAMP-AM is contingent on PLC- $\epsilon$ catalytic and Rap binding activities

Using the rescue protocol described for Fig. 7D, we sought to determine to what extent the catalytic and Rap binding activities of PLC- $\epsilon$  were important to the overall process by which CICR was facilitated by 8-pCPT-2'-O-Me-cAMP-AM. To this end,  $\beta$ -cells of PLC- $\epsilon$  KO mice were transduced with WT PLC- $\epsilon$  or mutant forms of PLC- $\epsilon$  that contained amino acid substitutions that rendered the enzyme catalytically dead (H1640L) or incapable of Rap binding (K2150E; Fig. 8A). This analysis revealed that WT PLC- $\epsilon$  rescued the action of 8-pCPT-2'-O-Me-cAMP-AM (0.3  $\mu$ M) to facilitate CICR, whereas no such rescue was measurable after transduction with either H1640L or K2150E PLC- $\epsilon$ . This outcome was the case even after raising the concentration of 8-pCPT-2'-O-Me-cAMP-AM to 1  $\mu$ M (Fig. 8B). Thus, the catalytic and Rap binding activities of PLC- $\epsilon$  are indispensable in order for PLC- $\epsilon$  to serve as an Epac2 effector with Ca<sup>2+</sup> mobilizing functions.

### Downregulation of Rap GTPase activity disrupts Epac2- but not PKA-regulated CICR

Since cAMP signals through Epac and Rap to activate PLC- $\epsilon$  in other cell types, it may be predicted that in  $\beta$ -cells of WT mice, the downregulation of Rap activity will uncouple Epac2 activation from the facilitation of CICR. This possibility was tested by transducing  $\beta$ -cells with a bicistronic adenovirus directing expression of EYFP and a RapGAP that is a GTPase activating protein and

that stimulates the conversion of Rap from an active GTP-bound form to an inactive GDP-bound form (Bos *et al.* 2007). We found that in conditions of UV flash photolysis in which  $\text{Ca}^{2+}$  was uncaged from NP-EGTA, the action of 8-pCPT-2'-O-Me-cAMP-AM ( $1 \mu\text{M}$ ) to facilitate CICR was abrogated in WT  $\beta$ -cells expressing RapGAP (Fig. 8C and D). This functional antagonism was highly selective, in that RapGAP failed to influence the ability of PKA activator 6-Bnz-cAMP-AM ( $1 \mu\text{M}$ ) to facilitate CICR (Fig. 8C and E).

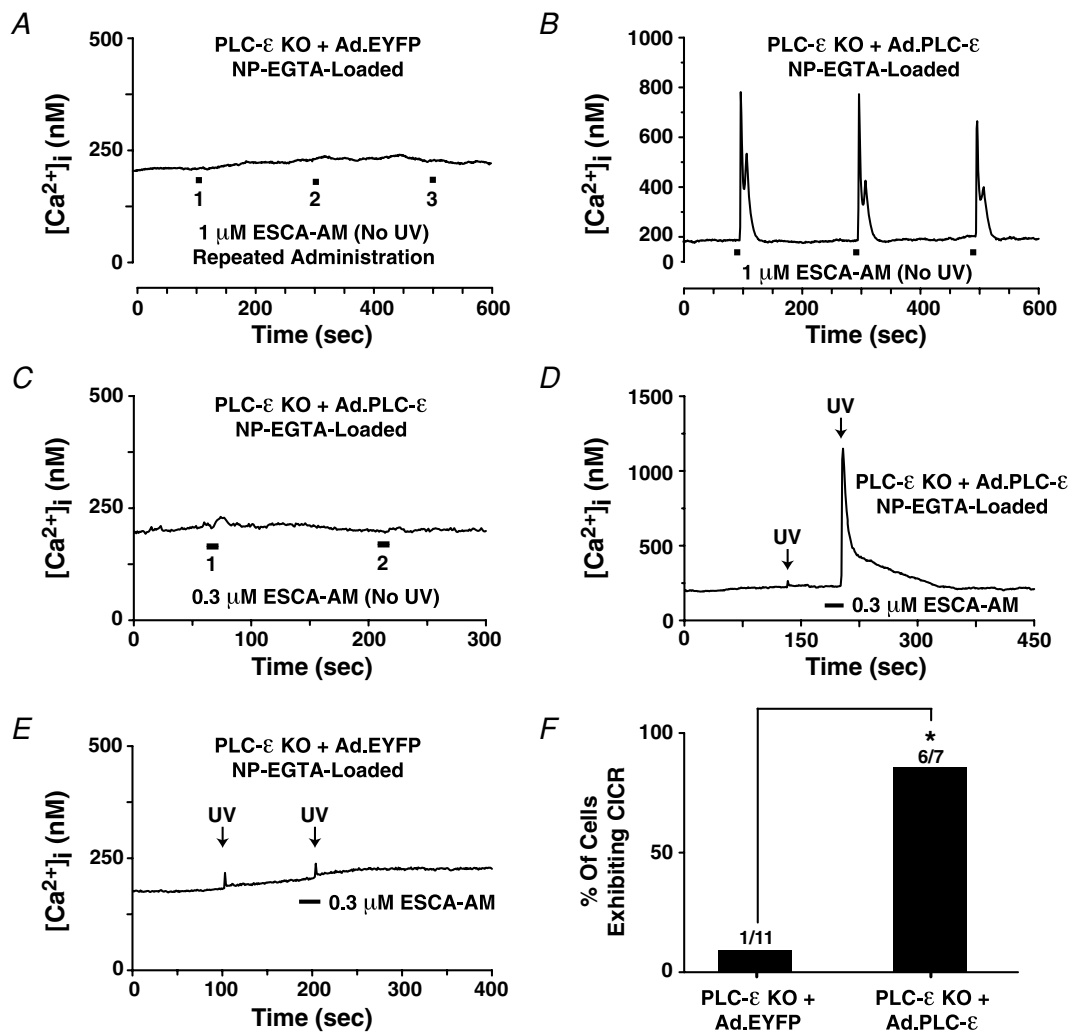


**Figure 7. Rescue of CICR by transduction with recombinant wild-type PLC- $\epsilon$**

A–C, 8-pCPT-2'-O-Me-cAMP-AM (ESCA-AM) tested in conditions of NP-EGTA loading but in the absence of UV flash photolysis for PLC- $\epsilon$  KO mouse  $\beta$ -cells expressing recombinant EYFP only (A) or EYFP and recombinant PLC- $\epsilon$  (Ad.PLC- $\epsilon$ ; B and C). Note that 8-pCPT-2'-O-Me-cAMP-AM was tested at  $1 \mu\text{M}$  (A and B) or  $0.3 \mu\text{M}$  (C). D, 8-pCPT-2'-O-Me-cAMP-AM ( $0.3 \mu\text{M}$ ) facilitated CICR triggered by the uncaging of  $\text{Ca}^{2+}$  in a PLC- $\epsilon$  KO mouse  $\beta$ -cell transduced with recombinant PLC- $\epsilon$ . E, transduction with EYFP only failed to rescue the action of 8-pCPT-2'-O-Me-cAMP-AM ( $0.3 \mu\text{M}$ ) to facilitate CICR in a PLC- $\epsilon$  KO mouse  $\beta$ -cell. F, population studies summarizing the ability of recombinant PLC- $\epsilon$  but not EYFP to rescue the action of 8-pCPT-2'-O-Me-cAMP-AM ( $0.3 \mu\text{M}$ ) in the CICR assay using PLC- $\epsilon$  KO mouse  $\beta$ -cells. \* $P < 0.001$ .

## Discussion

### Phospholipase C- $\epsilon$ is a novel Epac2- and Rap1-regulated phospholipase expressed in islet $\beta$ -cells

Although GLP-1R signal transduction in  $\beta$ -cells involves the cAMP-dependent activation of both PKA and Epac2, there exists controversy concerning whether or not GLP-1 can act independently of PKA and instead via Epac2 to stimulate  $\text{Ca}^{2+}$  signalling and insulin secretion (Renstrom *et al.* 1997; Bode *et al.* 1999; Kang *et al.* 2001; Eliasson *et al.* 2003; Gromada *et al.* 2004; Holz, 2004; Seino & Shibasaki, 2005; Thams *et al.* 2005; Hatakeyama *et al.* 2006, 2007; Kwan *et al.* 2007; Shibasaki *et al.* 2007;

Chepurny *et al.* 2010; Idevall-Hagren *et al.* 2010). In fact, only one published study clearly links GLP-1R activation to the Epac2-dependent stimulation of islet insulin secretion, as studied in mouse islets treated with Epac2 antisense deoxyoligonucleotides (Kashima *et al.* 2001). Furthermore, although Epac2 is reported to act through its immediate effector Rap1 GTPase to potentiate glucose-stimulated insulin secretion from mouse islets (Shibasaki *et al.* 2007), exactly how activated Rap1 promotes the  $\text{Ca}^{2+}$ -dependent exocytosis of insulin from  $\beta$ -cells has remained uncertain. Thus, the new findings presented here are significant in that we document the expression and functionality of a novel Epac2- and Rap1-regulated PLC- $\epsilon$ , the activation of which couples

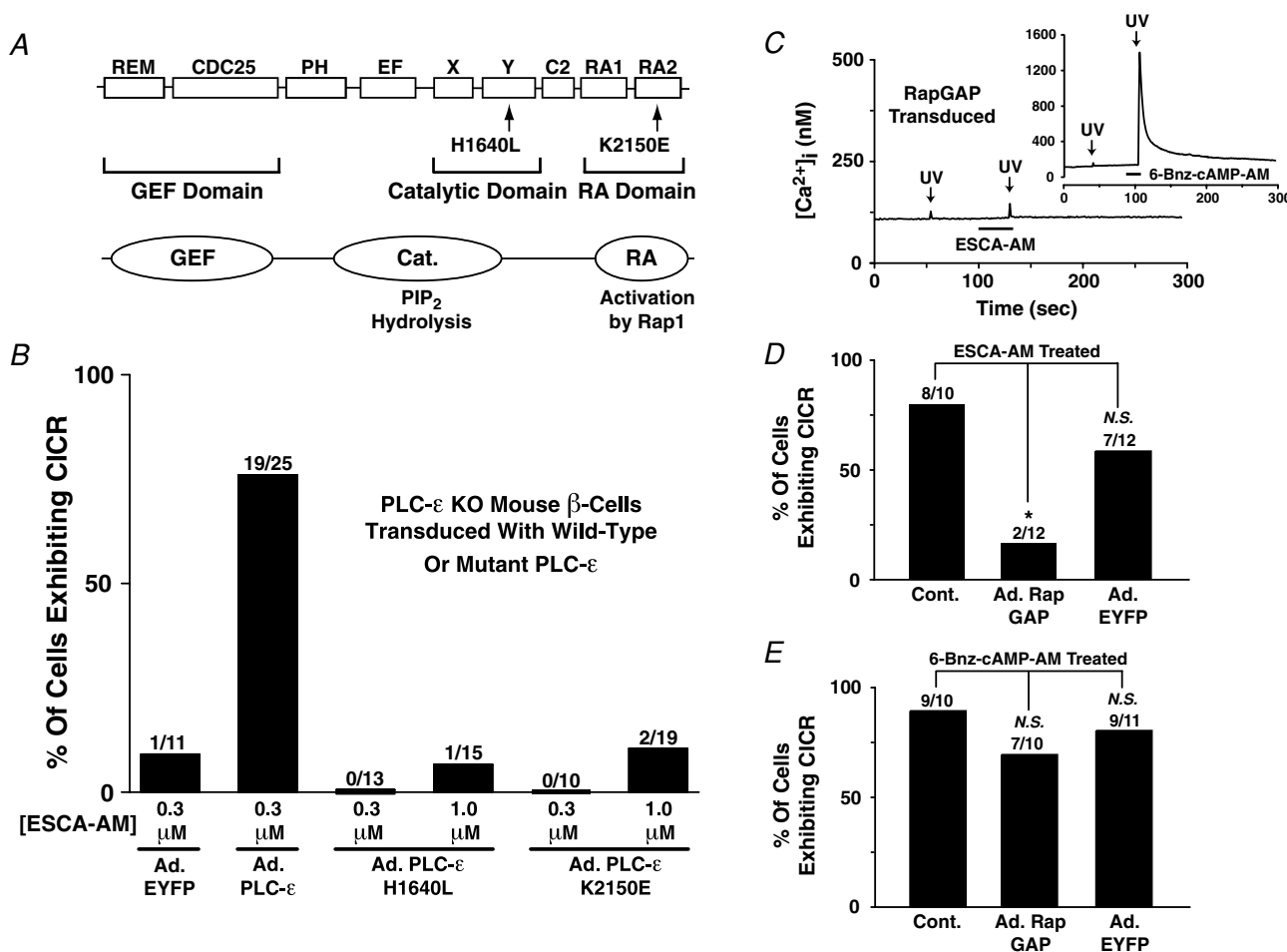


**Figure 8. Rap-regulated PLC- $\epsilon$  catalytic activity is required for the rescue of CICR**

*A*, domain structure of PLC- $\epsilon$  illustrating the H1640L and K2150E amino acid substitutions within the catalytic domain (Y-box) and the Rap Association 2 (RA2) domain, respectively. *B*, population studies of  $\beta$ -cells from PLC- $\epsilon$  KO mice illustrating the action of 8-pCPT-2'-O-Me-cAMP-AM (0.3 or 1  $\mu\text{M}$ ) to rescue CICR in PLC- $\epsilon$  KO mouse  $\beta$ -cells transduced with wild-type PLC- $\epsilon$  but not mutant forms of PLC- $\epsilon$  that lack phosphoinositide-specific catalytic activity (H1640L PLC- $\epsilon$ ) or the Rap binding function (K2150E PLC- $\epsilon$ ). *C*, transduction of WT mouse  $\beta$ -cells with RapGAP abrogated the action of 8-pCPT-2'-O-Me-cAMP-AM (1  $\mu\text{M}$ ) but not 6-Bnz-cAMP-AM (1  $\mu\text{M}$ ) to facilitate CICR. *D* and *E*, population studies summarizing the actions of 8-pCPT-2'-O-Me-cAMP-AM (1  $\mu\text{M}$ ) or 6-Bnz-cAMP-AM (1  $\mu\text{M}$ ) to facilitate or not facilitate CICR in WT mouse  $\beta$ -cells transduced with RapGAP or EYFP (negative control). \* $P < 0.001$ .

$\beta$ -cell GLP-1R occupancy to the facilitation of CICR that mobilizes intracellular  $\text{Ca}^{2+}$ . Given that an analogous mechanism of Epac2-regulated CICR is known to be coupled to  $\text{Ca}^{2+}$ -dependent exocytosis in human  $\beta$ -cells (Kang *et al.* 2003), and since the selective Epac activator 8-pCPT-2'-O-Me-cAMP-AM exerts a powerful insulin secretagogue action in both human and mouse islets (Chepurny *et al.* 2009, 2010; Kelley *et al.* 2009), it would appear that Epac2 and PLC- $\epsilon$  participate in  $\beta$ -cell stimulus–secretion coupling that is under the control of the GLP-1R.

### Unexpected molecular properties of CICR in mouse $\beta$ -cells

It is particularly surprising that we find that the Epac2-mediated  $\text{Ca}^{2+}$  mobilizing action of GLP-1R agonist exendin-4 requires expression of a phosphoinositide (PI) specific PLC- $\epsilon$  in mouse  $\beta$ -cells. This is unexpected because in earlier studies it was reported that GLP-1R agonists failed to stimulate  $^3\text{H}$ -inositol phosphate ( $^3\text{H}$ -IP) release from *myo*-[2- $^3\text{H}$ ]-inositol prelabelled rat islets and rat INS-1 insulin-secreting cells (Fridolf & Ahren, 1991; Widmann *et al.* 1994; Kang *et al.* 2003). Such negative findings concerning PI hydrolysis were interpreted to indicate that the  $\text{Ca}^{2+}$  mobilizing action of GLP-1 in  $\beta$ -cells was unrelated to PLC activation. Instead, it was proposed that GLP-1 mobilizes  $\text{Ca}^{2+}$  by sensitizing intracellular  $\text{Ca}^{2+}$  release channels to stimulatory effects of  $\text{IP}_3$  and  $\text{Ca}^{2+}$  (Gromada *et al.* 1995; Holz *et al.* 1999; Dyachok & Gylfe, 2004). Specifically, it was proposed that GLP-1 mobilizes  $\text{Ca}^{2+}$  in  $\beta$ -cells by promoting PKA-mediated phosphorylation of intracellular  $\text{Ca}^{2+}$  release channels, and that these channels correspond to  $\text{IP}_3$  receptors and ryanodine receptors (Gromada *et al.* 1995; Holz *et al.* 1999; Dyachok & Gylfe, 2004).

With these points in mind, it is significant that the new findings presented here do in fact confirm a PKA-mediated action of exendin-4 to mobilize  $\text{Ca}^{2+}$ , an action measurable in  $\beta$ -cells of Epac2 and PLC- $\epsilon$  KO mice. However, our studies of these same KO mice reveal a previously unrecognized  $\text{Ca}^{2+}$  mobilizing action of exendin-4, one that requires  $\beta$ -cell expression of Epac2 and PLC- $\epsilon$ . Since this PKA-independent action of exendin-4 is mimicked by 8-pCPT-2'-O-Me-cAMP-AM, and since the action of 8-pCPT-2'-O-Me-cAMP-AM is blocked by inhibitors of PKC and CaMKII, it could be that the GLP-1R does in fact signal through Epac2 and PLC- $\epsilon$  to stimulate PI hydrolysis and to modulate intracellular  $\text{Ca}^{2+}$  release channel function. This concept is consistent with previous reports that GLP-1 activated PKC in INS-1 cells (Suzuki *et al.* 2006), whereas 8-pCPT-2'-O-Me-cAMP-AM promoted PI hydrolysis in

INS-1 cells (Leech *et al.* 2010). Furthermore, GLP-1 was reported to stimulate  $^3\text{H}$ -IP release from COS cells expressing the recombinant GLP-1R (Wheeler *et al.* 1993), from frog oocytes expressing the recombinant GLP-1R (Gromada *et al.* 1998) and from mouse  $\beta\text{TC3}$  insulin-secreting cells expressing the endogenous GLP-1R (Gromada *et al.* 1995). In summary, a key issue that remains to be resolved concerns whether or not the Epac2-mediated action of exendin-4 to facilitate  $\beta$ -cell CICR results from PI hydrolysis and, if so, whether it is  $\text{IP}_3$  generation or PKC activation that controls the function of  $\text{IP}_3$  or ryanodine receptors.

### Potential physiological significance of CICR in mouse $\beta$ -cells

Since depolarization-induced  $\text{Ca}^{2+}$  influx is already well established to be a direct stimulus for insulin secretion (Eliasson *et al.* 2008), it is reasonable to question whether CICR is of major physiological significance to  $\beta$ -cell stimulus–secretion coupling. In fact, in one prior study of mouse  $\beta$ -cells, no coupling of CICR to exocytosis was measurable, and the emptying of ER  $\text{Ca}^{2+}$  stores by treatment with thapsigargin failed to reduce islet insulin secretion stimulated by glucose (Zhang *et al.* 2007). Unfortunately, the interpretation of this prior study is not clear-cut due to the fact that exocytosis was studied in conditions in which  $\beta$ -cells were not treated with cAMP-elevating agents. This is an important consideration because in the present study we found that in the absence of cAMP-elevating agents, CICR was rarely triggered in mouse  $\beta$ -cells. With these points in mind, we argue that an amplification mechanism exists for  $\beta$ -cell exocytosis, one that requires CICR and that is only operational when  $\beta$ -cells are treated with cAMP-elevating agents. This concept is based on prior studies in which cAMP was found to act through PKA to increase the size of a highly  $\text{Ca}^{2+}$ -sensitive pool of insulin secretory granules (Wan *et al.* 2004; Yang & Gillis, 2004). Specifically, we propose that in the absence of cAMP-elevating agents, exocytosis stimulated by glucose will be restricted to a small number of secretory granules that are co-localized with VDCCs at the plasma membrane. These secretory granules are predicted to undergo exocytosis in response to the large (10–20  $\mu\text{M}$ ) increase of  $[\text{Ca}^{2+}]_i$  that occurs at the inner mouths of VDCCs when these channels open in response to glucose metabolism-dependent membrane depolarization. In the presence of both GLP-1 and glucose, cAMP will act through PKA to increase the number of highly  $\text{Ca}^{2+}$ -sensitive secretory granules that are located near the plasma membrane, but that are not docked and co-localized with VDCCs. Thus, in conditions in which Epac2 is activated and CICR is facilitated, a more modest (500 nM to 2.0  $\mu\text{M}$ ) and globally distributed increase

of  $[Ca^{2+}]_i$  will trigger the exocytosis of a much larger number of secretory granules present within the highly  $Ca^{2+}$ -sensitive pool. This model is compatible with our previous study demonstrating an ability of CICR to initiate 'summing' exocytosis, as detected using the methods of carbon fibre amperometry (Kang & Holz, 2003).

## Conclusion

Although the new findings presented here document a mechanism of GLP-1R-regulated CICR in  $\beta$ -cells, it is noteworthy that GLP-1 receptors are also expressed in the heart, and in fact GLP-1R agonists are under investigation for their potential usefulness in the treatment of cardiovascular diseases (Fields *et al.* 2009; Treiman *et al.* 2010). Furthermore, the heart also contains a receptor for the metabolite of GLP-1 designated as GLP-1 (9–36)-amide and, as is the case for GLP-1, this metabolite is capable of stimulating cAMP production in cardiomyocytes (Ban *et al.* 2008, 2010). Given that the  $\beta$ -cell GLP-1R signals through Epac2 to facilitate CICR, and in view of the fact that Epac-selective cAMP analogues act via Epac1 and possibly Epac2 to regulate multiple parameters of cardiomyocyte function (Morel *et al.* 2005; Somekawa *et al.* 2005; Oestreich *et al.* 2007, 2009; Pereira *et al.* 2007; Hothi *et al.* 2008; Métrich *et al.* 2008, 2010; Cazorla *et al.* 2009; Duquesnes *et al.* 2010; Mangmool *et al.* 2010), it could be that GLP-1R agonists currently in use for the treatment of type 2 diabetes mellitus might have the additional ability to act in an Epac-mediated manner to exert therapeutically important actions in the myocardium.

## References

- Ban K, Kim KH, Cho CK, Sauvé M, Diamandis EP, Backx PH, Drucker DJ & Husain M (2010). Glucagon-like peptide (GLP)-1(9–36)amide-mediated cytoprotection is blocked by exendin(9–39) yet does not require the known GLP-1 receptor. *Endocrinology* **151**, 1520–1531.
- Ban K, Noyan-Ashraf MH, Hofer J, Bolz SS, Drucker DJ & Husain M (2008). Cardioprotective and vasodilatory actions of glucagon-like peptide 1 receptor are mediated through both glucagon-like peptide 1 receptor-dependent and -independent pathways. *Circulation* **117**, 2340–2350.
- Beauvois MC, Arredouani A, Jonas JC, Rolland JF, Schuit F, Henquin JC & Gilon P (2004). Atypical  $Ca^{2+}$ -induced  $Ca^{2+}$  release from a SERCA3-dependent  $Ca^{2+}$  pool of the endoplasmic reticulum in mouse pancreatic beta cells. *J Physiol* **559**, 141–156.
- Bode HP, Moormann B, Dabew R & Goke B (1999). Glucagon-like peptide-1 elevates cytosolic calcium in pancreatic  $\beta$ -cells independently of protein kinase A. *Endocrinology* **140**, 3919–3927.
- Bos JL, Rehmann H & Wittinghofer A (2007). GEFs and GAPs: critical elements in the control of small G proteins. *Cell* **129**, 865–877.
- Calcraft PJ, Ruas M, Pan Z, Cheng X, Arredouani A, Hao X, Tang J, Rietdorf K, Teboul L, Chuang KT, Lin P, Xiao R, Wang C, Zhu Y, Lin Y, Wyatt CN, Parrington J, Ma J, Evans AM, Galione A & Zhu MX (2009). NAADP mobilizes calcium from acidic organelles through two-pore channels. *Nature* **459**, 596–600.
- Cazorla O, Lucas A, Poirier F, Lacampagne A & Lezoualc'h F (2009). The cAMP binding protein Epac regulates cardiac myofilament function. *Proc Natl Acad Sci U S A* **106**, 14144–14149.
- Chepurny OG, Kelley GG, Dzhura I, Leech CA, Roe MW, Dzhura E, Li X, Schwede F, Genieser HG & Holz GG (2010). PKA-dependent potentiation of glucose-stimulated insulin secretion by Epac activator 8-pCPT-2'-O-Me-cAMP-AM in human islets of Langerhans. *Am J Physiol Endocrinol Metab* **298**, E622–E633.
- Chepurny OG, Leech CA, Kelley GG, Dzhura I, Dzhura E, Li X, Rindler MJ, Schwede F, Genieser HG & Holz GG (2009). Enhanced Rap1 activation and insulin secretagogue properties of an acetoxymethyl ester of an Epac-selective cyclic AMP analog in rat INS-1 cells: studies with 8-pCPT-2'-O-Me-cAMP-AM. *J Biol Chem* **284**, 10728–10736.
- Citro S, Malik S, Oestreich EA, Radeff-Huang J, Kelley GG, Smrcka AV & Brown JH (2007). Phospholipase  $C\epsilon$  is a nexus for Rho and Rap-mediated G protein-coupled receptor-induced astrocyte proliferation. *Proc Natl Acad Sci U S A* **104**, 15543–15548.
- de Rooij J, Zwartkruis FJ, Verheijen MH, Cool RH, Nijman SM, Wittinghofer A & Bos JL (1998). Epac is a Rap1 guanine-nucleotide-exchange factor directly activated by cyclic AMP. *Nature* **396**, 474–477.
- Drummond GB (2009). Reporting ethical matters in *The Journal of Physiology*: standards and advice. *J Physiol* **587**, 713–719.
- Duquesnes N, Derangeon M, Métrich M, Lucas A, Mateo P, Li L, Morel E, Lezoualc'h F & Crozatier B (2010). Epac stimulation induces rapid increases in connexin43 phosphorylation and function without preconditioning effect. *Pflugers Arch* **460**, 7317–41.
- Dyachok O & Gylfe E (2004).  $Ca^{2+}$ -induced  $Ca^{2+}$  release via inositol 1,4,5-trisphosphate receptors is amplified by protein kinase A. *J Biol Chem* **279**, 45455–45461.
- Eliasson L, Abdulkader F, Braun M, Galvanovskis J, Hoppa MB & Rorsman P (2008). Novel aspects of the molecular mechanisms controlling insulin secretion. *J Physiol* **586**, 3313–3324.
- Eliasson L, Ma X, Renstrom E, Barg S, Berggren PO, Galvanovskis J, Gromada J, Jing X, Lundquist I, Salehi A, Sewing S & Rorsman P (2003). SUR1 regulates PKA-independent cAMP-induced granule priming in mouse pancreatic B-cells. *J Gen Physiol* **121**, 181–197.
- Enyeart JA, Liu H & Enyeart JJ (2010). cAMP analogs and their metabolites enhance TREK-1 mRNA and  $K^+$  current expression in adrenocortical cells. *Mol Pharmacol* **77**, 469–482.
- Fields AV, Patterson B, Karnik AA & Shannon RP (2009). Glucagon-like peptide-1 and myocardial protection: more than glycemic control. *Clin Cardiol* **32**, 236–243.

- Fridolf T & Ahren B (1991). GLP-1-(7–36)-amide stimulates insulin secretion in rat islets: studies on the mode of action. *Diabetes Res* **16**, 185–191.
- Gromada J, Anker C, Bokvist K, Knudsen LB & Wahl P (1998). Glucagon-like peptide-1 receptor expression in *Xenopus* oocytes stimulates inositol trisphosphate-dependent intracellular  $\text{Ca}^{2+}$  mobilization. *FEBS Lett* **425**, 277–280.
- Gromada J, Brock B, Schmitz O & Rorsman P (2004). Glucagon-like peptide-1: regulation of insulin secretion and therapeutic potential. *Basic Clin Pharmacol Toxicol* **95**, 252–262.
- Gromada J, Dissing S, Bokvist K, Renstrom E, Frokjaer-Jensen J, Wulff BS & Rorsman P (1995). Glucagon-like peptide-1 increases cytoplasmic  $\text{Ca}^{2+}$  in insulin-secreting betaTC3 cells by enhancement of intracellular  $\text{Ca}^{2+}$  mobilization. *Diabetes* **44**, 767–774.
- Gryniewicz G, Poenie M & Tsien RY (1985). A new generation of  $\text{Ca}^{2+}$  indicators with greatly improved fluorescence properties. *J Biol Chem* **260**, 3440–3450.
- Hatakeyama H, Kishimoto T, Nemoto T, Kasai H & Takahashi N (2006). Rapid glucose sensing by protein kinase A for insulin exocytosis in mouse pancreatic islets. *J Physiol* **570**, 271–282.
- Hatakeyama H, Takahashi N, Kishimoto T, Nemoto T & Kasai H (2007). Two cAMP-dependent pathways differentially regulate exocytosis of large dense-core and small vesicles in mouse  $\beta$ -cells. *J Physiol* **582**, 1087–1098.
- Holz GG (2004). Epac: a new cAMP-binding protein in support of glucagon-like peptide-1 receptor-mediated signal transduction in the pancreatic  $\beta$ -cell. *Diabetes* **53**, 5–13.
- Holz GG, Chepurny OG & Schwede F (2008). Epac-selective cAMP analogs: new tools with which to evaluate the signal transduction properties of cAMP-regulated guanine nucleotide exchange factors. *Cell Signal* **20**, 10–20.
- Holz GG, Kuhlreiber WM & Habener JF (1993). Pancreatic  $\beta$ -cells are rendered glucose competent by the insulinotropic hormone glucagon-like peptide-1-(7–37). *Nature* **361**, 362–365.
- Holz GG, Leech CA, Heller RS, Castonguay M & Habener JF (1999). cAMP-dependent mobilization of intracellular  $\text{Ca}^{2+}$  stores by activation of ryanodine receptors in pancreatic  $\beta$ -cells. A  $\text{Ca}^{2+}$  signaling system stimulated by the insulinotropic hormone glucagon-like peptide-1-(7–37). *J Biol Chem* **274**, 14147–14156.
- Hothi SS, Gurung IS, Heathcote JC, Zhang Y, Booth SW, Skepper JN, Grace AA & Huang CL (2008). Epac activation, altered calcium homeostasis and ventricular arrhythmogenesis in the murine heart. *Pflugers Arch* **457**, 253–270.
- Idevall-Hagren O, Barg S, Gylfe E & Tengholm A (2010). cAMP mediators of pulsatile insulin secretion from glucose-stimulated single  $\beta$ -cells. *J Biol Chem* **285**, 23007–23018.
- Islam MS, Rorsman P & Berggren PO (1992).  $\text{Ca}^{2+}$ -induced  $\text{Ca}^{2+}$  release in insulin-secreting cells. *FEBS Lett* **296**, 287–291.
- Kang G, Chepurny OG & Holz GG (2001). cAMP-regulated guanine nucleotide exchange factor II (Epac2) mediates  $\text{Ca}^{2+}$ -induced  $\text{Ca}^{2+}$  release in INS-1 pancreatic  $\beta$ -cells. *J Physiol* **536**, 375–385.
- Kang G, Chepurny OG, Rindler MJ, Collis L, Chepurny Z, Li WH, Harbeck M, Roe MW & Holz GG (2005). A cAMP and  $\text{Ca}^{2+}$  coincidence detector in support of  $\text{Ca}^{2+}$ -induced  $\text{Ca}^{2+}$  release in mouse pancreatic  $\beta$  cells. *J Physiol* **566**, 173–188.
- Kang G & Holz GG (2003). Amplification of exocytosis by  $\text{Ca}^{2+}$ -induced  $\text{Ca}^{2+}$  release in INS-1 pancreatic  $\beta$  cells. *J Physiol* **546**, 175–189.
- Kang G, Joseph JW, Chepurny OG, Monaco M, Wheeler MB, Bos JL, Schwede F, Genieser HG & Holz GG (2003). Epac-selective cAMP analog 8-pCPT-2'-O-Me-cAMP as a stimulus for  $\text{Ca}^{2+}$ -induced  $\text{Ca}^{2+}$  release and exocytosis in pancreatic  $\beta$  cells. *J Biol Chem* **278**, 8279–8285.
- Kashima Y, Miki T, Shibasaki T, Ozaki N, Miyazaki M, Yano H & Seino S (2001). Critical role of cAMP-GEFII-Rim2 complex in incretin-potentiated insulin secretion. *J Biol Chem* **276**, 46046–46053.
- Kawasaki H, Springett GM, Mochizuki N, Toki S, Nakaya M, Matsuda M, Housman DE & Graybiel AM (1998). A family of cAMP-binding proteins that directly activate Rap1. *Science* **282**, 2275–2279.
- Kelley GG, Chepurny OG, Schwede F, Genieser HG, Leech CA, Roe MW, Li X, Dzhura I, Dzhura E, Afshari P & Holz GG (2009). Glucose-dependent potentiation of mouse islet insulin secretion by Epac activator 8-pCPT-2'-O-Me-cAMP-AM. *Islets* **1**, 260–265.
- Kelley GG, Reks SE, Ondrako JM & Smrcka AV (2001). Phospholipase C $\epsilon$ : a novel Ras effector. *EMBO J* **20**, 743–754.
- Kelley GG, Reks SE & Smrcka AV (2004). Hormonal regulation of phospholipase C $\epsilon$  through distinct and overlapping pathways involving G<sub>12</sub> and Ras family G-proteins. *Biochem J* **378**, 129–139.
- Kim BJ, Park KH, Yim CY, Takasawa S, Okamoto H, Im MJ & Kim UH (2008). Generation of nicotinic acid adenine dinucleotide phosphate and cyclic ADP-ribose by glucagon-like peptide-1 evokes  $\text{Ca}^{2+}$  signal that is essential for insulin secretion in mouse pancreatic islets. *Diabetes* **57**, 868–878.
- Kwan EP, Xie L, Sheu L, Ohtsuka T & Gaisano HY (2007). Interaction between Munc13–1 and RIM is critical for glucagon-like peptide-1-mediated rescue of exocytotic defects in Munc13–1-deficient pancreatic  $\beta$ -cells. *Diabetes* **56**, 2579–2588.
- Laxman S, Riechers A, Sadilek M, Schwede F & Beavo JA (2006). Hydrolysis products of cAMP analogs cause transformation of *Trypanosoma brucei* from slender to stumpy-like forms. *Proc Natl Acad Sci U S A* **103**, 19194–19199.
- Leech CA, Dzhura I, Chepurny OG, Schwede F, Genieser HG & Holz GG (2010). Facilitation of beta-cell KATP channel sulfonylurea sensitivity by a cAMP analog selective for the cAMP-regulated guanine nucleotide exchange factor Epac. *Islets* **2**, 72–81.
- Lemmens R, Larsson O, Berggren PO & Islam MS (2001).  $\text{Ca}^{2+}$ -induced  $\text{Ca}^{2+}$  release from the endoplasmic reticulum amplifies the  $\text{Ca}^{2+}$  signal mediated by activation of voltage-gated L-type  $\text{Ca}^{2+}$  channels in pancreatic  $\beta$ -cells. *J Biol Chem* **276**, 9971–9977.
- Livak KJ & Schmittgen TD (2001). Analysis of relative gene expression data using real-time quantitative PCR and the  $2^{-\Delta\Delta C_T}$  method. *Methods* **25**, 402–408.

- Lopez I, Mak EC, Ding J, Hamm HE & Lomasney JW (2001). A novel bifunctional phospholipase C that is regulated by  $G\alpha_{12}$  and stimulates the Ras/mitogen-activated protein kinase pathway. *J Biol Chem* **276**, 2758–2765.
- Mangmool S, Shukla AK & Rockman HA (2010).  $\beta$ -Arrestin-dependent activation of  $Ca^{2+}$ /calmodulin kinase II after  $\beta_1$ -adrenergic receptor stimulation. *J Cell Biol* **189**, 573–587.
- Métrich M, Laurent AC, Breckler M, Duquesnes N, Hmitou I, Courillau D, Blondeau JP, Crozatier B, Lezoualc'h F & Morel E (2010). Epac activation induces histone deacetylase nuclear export via a Ras-dependent signalling pathway. *Cell Signal* **22**, 1459–1468.
- Métrich M, Lucas A, Gastineau M, Samuel JL, Heymes C, Morel E & Lezoualc'h F (2008). Epac mediates  $\beta$ -adrenergic receptor-induced cardiomyocyte hypertrophy. *Circ Res* **102**, 959–965.
- Morel E, Marcantoni A, Gastineau M, Birkedal R, Rochais F, Garnier A, Lompré AM, Vandecasteele G & Lezoualc'h F (2005). cAMP-binding protein Epac induces cardiomyocyte hypertrophy. *Circ Res* **97**, 1296–1304.
- Naylor E, Arredouani A, Vasudevan SR, Lewis AM, Parkesh R, Mizote A, Rosen D, Thomas JM, Izumi M, Ganesan A, Galione A & Churchill GC (2009). Identification of a chemical probe for NAADP by virtual screening. *Nat Chem Biol* **5**, 220–226.
- Oestreich EA, Malik S, Goonasekera SA, Blaxall BC, Kelley GG, Dirksen RT & Smrcka AV (2009). Epac and phospholipase  $C\epsilon$  regulate  $Ca^{2+}$  release in the heart by activation of protein kinase  $C\epsilon$  and calcium-calmodulin kinase II. *J Biol Chem* **284**, 1514–1522.
- Oestreich EA, Wang H, Malik S, Kaproth-Joslin KA, Blaxall BC, Kelley GG, Dirksen RT & Smrcka AV (2007). Epac-mediated activation of phospholipase  $C\epsilon$  plays a critical role in  $\beta$ -adrenergic receptor-dependent enhancement of  $Ca^{2+}$  mobilization in cardiac myocytes. *J Biol Chem* **282**, 5488–5495.
- Ozaki N, Shibasaki T, Kashima Y, Miki T, Takahashi K, Ueno H, Sunaga Y, Yano H, Matsuura Y, Iwanaga T, Takai Y & Seino S (2000). cAMP-GEFII is a direct target of cAMP in regulated exocytosis. *Nat Cell Biol* **2**, 805–811.
- Pereira L, Métrich M, Fernández-Velasco M, Lucas A, Leroy J, Perrier R, Morel E, Fischmeister R, Richard S, Bénitah JP, Lezoualc'h F & Gómez AM (2007). The cAMP binding protein Epac modulates  $Ca^{2+}$  sparks by a  $Ca^{2+}$ /calmodulin kinase signalling pathway in rat cardiac myocytes. *J Physiol* **583**, 685–694.
- Renstrom E, Eliasson L & Rorsman P (1997). Protein kinase A-dependent and -independent stimulation of exocytosis by cAMP in mouse pancreatic B-cells. *J Physiol* **502**, 105–118.
- Schmidt M, Evellin S, Weernink PA, von Dorp F, Rehmann H, Lomasney JW & Jakobs KH (2001). A new phospholipase C-calcium signalling pathway mediated by cyclic AMP and a Rap GTPase. *Nat Cell Biol* **3**, 1020–1024.
- Seino S & Shibasaki T (2005). PKA-dependent and PKA-independent pathways for cAMP-regulated exocytosis. *Physiol Rev* **85**, 1303–1342.
- Shibasaki T, Takahashi H, Miki T, Sunaga Y, Matsumura K, Yamanaka M, Zhang C, Tamamoto A, Satoh T, Miyazaki J & Seino S (2007). Essential role of Epac2/Rap1 signaling in regulation of insulin granule dynamics by cAMP. *Proc Natl Acad Sci U S A* **104**, 19333–19338.
- Somekawa S, Fukuhara S, Nakaoka Y, Fujita H, Saito Y & Mochizuki N (2005). Enhanced functional gap junction neofunction by protein kinase A-dependent and Epac-dependent signals downstream of cAMP in cardiac myocytes. *Circ Res* **97**, 655–662.
- Song C, Hu CD, Masago M, Kariyai K, Yamawaki-Kataoka Y, Shibatohe M, Wu D, Satoh T & Kataoka T (2001). Regulation of a novel human phospholipase C, PLC $\epsilon$ , through membrane targeting by Ras. *J Biol Chem* **276**, 2752–2757.
- Song C, Satoh T, Edamatsu H, Wu D, Tadano M, Gao X & Kataoka T (2002). Differential roles of Ras and Rap1 in growth factor-dependent activation of phospholipase  $C\epsilon$ . *Oncogene* **21**, 8105–8113.
- Suzuki Y, Zhang H, Saito N, Kojima I, Urano T & Mogami H (2006). Glucagon-like peptide 1 activates protein kinase C through  $Ca^{2+}$ -dependent activation of phospholipase C in insulin-secreting cells. *J Biol Chem* **281**, 28499–28507.
- Thams P, Anwar MR & Capito K (2005). Glucose triggers protein kinase A-dependent insulin secretion in mouse pancreatic islets through activation of the  $K^{+}_{ATP}$  channel-dependent pathway. *Eur J Endocrinol* **152**, 671–677.
- Treiman M, Elvekjaer M, Engström T & Jensen JS (2010). Glucagon-like peptide 1—a cardiologic dimension. *Trends Cardiovasc Med* **20**, 8–12.
- Tu W, Xu X, Peng L, Zhong X, Zhang W, Soundarapandian MM, Balel C, Wang M, Jia N, Zhang W, Lew F, Chan SL, Chen Y & Lu Y (2010). DAPK1 interaction with NMDA receptor NR2B subunits mediates brain damage in stroke. *Cell* **140**, 222–234.
- Vliem MJ, Ponsioen B, Schwede F, Pannekoek WJ, Riedl J, Kooistra MR, Jalink K, Genieser HG, Bos JL & Rehmann H (2008). 8-pCPT-2'-O-Me-cAMP-AM: an improved Epac-selective cAMP analogue. *Chembiochem* **9**, 2052–2054.
- Wan Q-F, Dong Y, Yang H, Lou X, Ding J & Xu T (2004). Protein kinase activation increases insulin secretion by sensitizing the secretory machinery to  $Ca^{2+}$ . *J Gen Physiol* **124**, 653–662.
- Wang H, Oestreich EA, Maekawa N, Bullard TA, Vikstrom KL, Dirksen RT, Kelley GG, Blaxall BC & Smrcka AV (2005). Phospholipase  $C\epsilon$  modulates  $\beta$ -adrenergic receptor-dependent cardiac contraction and inhibits cardiac hypertrophy. *Circ Res* **97**, 1305–1313.
- Wheeler MB, Lu M, Dillon JS, Leng XH, Chen C & Boyd AE 3rd (1993). Functional expression of the rat glucagon-like peptide-I receptor, evidence for coupling to both adenylyl cyclase and phospholipase-C. *Endocrinology* **133**, 57–62.
- Widmann C, Bürki E, Dolci W & Thorens B (1994). Signal transduction by the cloned glucagon-like peptide-1 receptor: comparison with signaling by the endogenous receptors of beta cell lines. *Mol Pharmacol* **45**, 1029–1035.
- Yang Y & Gillis KD (2004). A highly  $Ca^{2+}$ -sensitive pool of granules is regulated by glucose and protein kinases in insulin-secreting INS-1 cells. *J Gen Physiol* **124**, 641–651.

Zhang Q, Bengtsson M, Partridge C, Salehi A, Braun M, Cox R, Eliasson L, Johnson PR, Renström E, Schneider T, Berggren PO, Göpel S, Ashcroft FM & Rorsman P (2007). R-type  $\text{Ca}^{2+}$  channel-evoked CICR regulates glucose-induced somatostatin secretion. *Nat Cell Biol* **9**, 453–460.

#### Author contributions

All authors contributed to the conception and design of the study, analysis and interpretation of data, drafting the article,

revising it critically for important intellectual content and final approval of the version to be published.

#### Acknowledgements

We wish to thank Dr. Frank Schwede of the BIOLOG Life Sci. Inst. for the gift of cAMP analogs. Funding was provided by the National Institutes of Health (DK045817, DK069575 to G.G.H.; DK074966 to M.W.R.; NS5051383, AG033282 to Y.L.; and R01GM053536 to A.V.S.) and the American Diabetes Association (Research Award to C.A.L.).

# Supplemental Material

## Epac2-dependent mobilization of intracellular Ca<sup>2+</sup> by GLP-1 receptor agonist Exendin-4 is disrupted in beta cells of PLC-ε knockout mice

---

Igor Dzhura<sup>1</sup>, Oleg G. Chepurny<sup>1</sup>, Grant G. Kelley<sup>1,2</sup>, Colin A. Leech<sup>1</sup>, Michael W. Roe<sup>1,3</sup>, Elvira Dzhura<sup>1</sup>, Parisa Afshari<sup>1</sup>, Sundeep Malik<sup>4</sup>, Michael J. Rindler<sup>5</sup>, Xu X<sup>6</sup>, Youming Lu<sup>6</sup>, Alan V. Smrcka<sup>4</sup>, and George G. Holz<sup>1,2,7</sup>

Departments of Medicine<sup>1</sup>, Pharmacology<sup>2</sup>, and Cell Biology<sup>3</sup>, State University of New York Upstate Medical University, Syracuse, NY, USA

<sup>4</sup>Department of Pharmacology and Physiology, University of Rochester School of Medicine, Rochester, NY, USA

<sup>5</sup>Department of Cell Biology, New York University School of Medicine, New York, NY

<sup>6</sup>Departments of Neurology and Neuroscience, Louisiana State University, Health Science Center, School of Medicine, New Orleans, LA, USA

<sup>7</sup>Corresponding Author:

George G. Holz, Ph.D.  
Professor of Medicine and Pharmacology  
SUNY Upstate Medical University  
IHP 4310  
505 Irving Avenue  
Syracuse, NY 13210  
Tel. 315-464-9841  
Fax 315-464-1566  
E-mail: holzg@upstate.edu

### Supplemental Material Includes:

Detailed Methods

3 Figures + 3 Legends

## **Detailed Methods**

### **Genotyping of Epac2 knockout mice**

Genotyping of wild-type and Epac2 knockout mice was performed using an Extract-N-Amp Tissue PCR Kit (Sigma-Aldrich) in order to obtain DNA from tail biopsies. The PCR primer pair used to confirm the wild-type *RAPGEF4* allele was: forward, 5'-CCTCATCCTAGCTGCCTGTAAG-3'; reverse, 5'-ACATGTAAATCACACAAGGTG-3'. To confirm incorporation of the targeting vector within *RAPGEF4* (Fig. 3A), the PCR primer pair consisted of a forward primer that annealed to the targeting vector and that corresponded to 5'-CTTGCAAATGGCGTACTTAA-3'. This forward primer was used in combination with the same 5'-ACATGTAAATCACACAAGGTG-3' reverse primer used to genotype the wild-type *RAPGEF4* allele (Fig. 3B, *left panel*).

The gene trap approach resulted in the insertion of the transgene within intron 1 of *RAPGEF4* so that transcription of the mutant *RAPGEF4* allele generated two mRNA transcripts (Fig. 3A of the main manuscript). To test for insertion of the transgene, we performed RT-PCR using a primer pair designed to amplify the cDNA that corresponds to mRNA spanning exons 1-4 of the wild-type allele. This primer pair failed to generate a PCR product in Epac2 knockout mice, but did amplify a PCR product in the wild-type mice (Fig. 3B, *right panel*). This primer pair consisted of: forward, 5'-GCGCACGCTGCACACTCTCA-3'; reverse, 5'-CCGCATCCTGGTGACTGCTGG-3'.

Knockout of Epac2 protein expression was achieved as a consequence of the incorporation of multiple translational stop codons within multiple reading frames of the transcript that contains the mRNA sequence corresponding to all exons of *RAPGEF4* located 3' to the insertion of the transgene (Fig. 3A). Thus, in both the wild-type and Epac2 knockout mice, RT-PCR generated PCR products when amplifying between exons 4 and 5 (Fig. 3B, *right panel*). The primer pair

used to generate this PCR product was: forward, 5'-CGCCATGCAACCATCGTTACC-3', reverse, 5'-GAGCCCGTTTCCATAACACC-3'.

Confirmation that Epac2 knockout mice failed to express Epac2 protein was obtained by performing Western blot analysis of mouse brain (Fig. 3C). For this purpose, the primary antiserum was a 1:100 dilution of a mouse monoclonal (5B1) antibody (Cell Signaling Tech., Danvers, MA), and the secondary antiserum was a 1:5,000 dilution of a goat anti-mouse horseradish peroxidase (HRP) conjugated IgG (Sigma-Aldrich). Enhanced chemiluminescence (ECL) detection was performed using a Pierce Pico ECL kit (Thermo Scientific).

### **Detection of Epac2 expression in islets**

For Western blot detection of Epac2 in human islet lysates, the primary antiserum was either a 1:100 dilution of mouse monoclonal (5B1) antibody or a 1:100 dilution of an affinity-purified polyclonal antiserum that was generated by a commercial source (FabGennix Inc., Frisco, TX) after immunization of rabbits with a KLH conjugated synthetic peptide corresponding to amino acid residues 743-761 (CPREQFDSLTPLEQEGPT) of mouse Epac2 (Swissprot Accession No. Q9EQZ6; Ozaki *et al.* 2000). This same epitope is present in both human Epac2 (Q8WZA2) and rat Epac2 (Q9Z1C7). For immunoblots using the anti-Epac2 monoclonal antibody, the secondary antiserum was a 1:5,000 dilution of a goat anti-mouse horseradish peroxidase (HRP) conjugated IgG. For immunoblots using the anti-Epac2 polyclonal antiserum, the secondary antiserum was a 1:10,000 dilution of a goat anti-rabbit HRP conjugated IgG.

## **Figure Legends**

### **Figure 1. 8-pCPT-2'-O-Me-cAMP-AM does not activate PKA in mouse islets, whereas CICR is facilitated by the hydrolysis-resistant Epac activator Sp-8-pCPT-2'-O-Me-cAMPS**

*A*, wild-type mouse islets were exposed to 8-pCPT-2'-O-Me-cAMP-AM for 30 min and lysates of these islets were then prepared. To each lysate was added a fluorescent PepTag derivative of the PKA substrate Kemptide [LRRASLG]. The unphosphorylated and phosphorylated forms of Kemptide were then resolved on the basis of their differential electrophoretic mobilities on an agarose gel. This analysis demonstrated that 1-10  $\mu$ M of 8-pCPT-2'-O-Me-cAMP-AM failed to activate PKA, as determined by the low levels of phosphate incorporation into Kemptide (P-Kemptide). However, 6-Bnz-cAMP-AM (10  $\mu$ M) did activate PKA, and this effect was blocked by co-treatment of islets with H-89 (10  $\mu$ M). For this assay, the negative control (- Control) was a reaction mixture to which no islet lysate was added, and the positive control (+ Control) was a reaction mixture containing no islet lysate but to which was added purified recombinant PKA catalytic subunit. *B*, population studies characterizing the dose-dependent action of hydrolysis-resistant 8-pCPT-2'-O-Me-cAMPS to facilitate CICR in wild-type mouse beta cells. Over each histogram bar is indicated a fraction in which the numerator is the number of cells exhibiting CICR, and the denominator is the number of cells tested.

### **Figure 2. Contrasting efficacies of thapsigargin and bafilomycin as inhibitors of CICR**

*A-B*, application of thapsigargin (1  $\mu$ M) to mouse beta cells stimulated a slow transient increase of  $[Ca^{2+}]_c$  and subsequently blocked the action of 8-pCPT-2'-O-Me-cAMP-AM (ESCA-AM, 1  $\mu$ M) and 6-Bnz-cAMP-AM (1  $\mu$ M) to facilitate CICR in response to the UV flash photolysis-catalyzed uncaging of  $Ca^{2+}$  (UV). *C-D*, bafilomycin (1  $\mu$ M) stimulated a slow transient increase of  $[Ca^{2+}]_c$  in

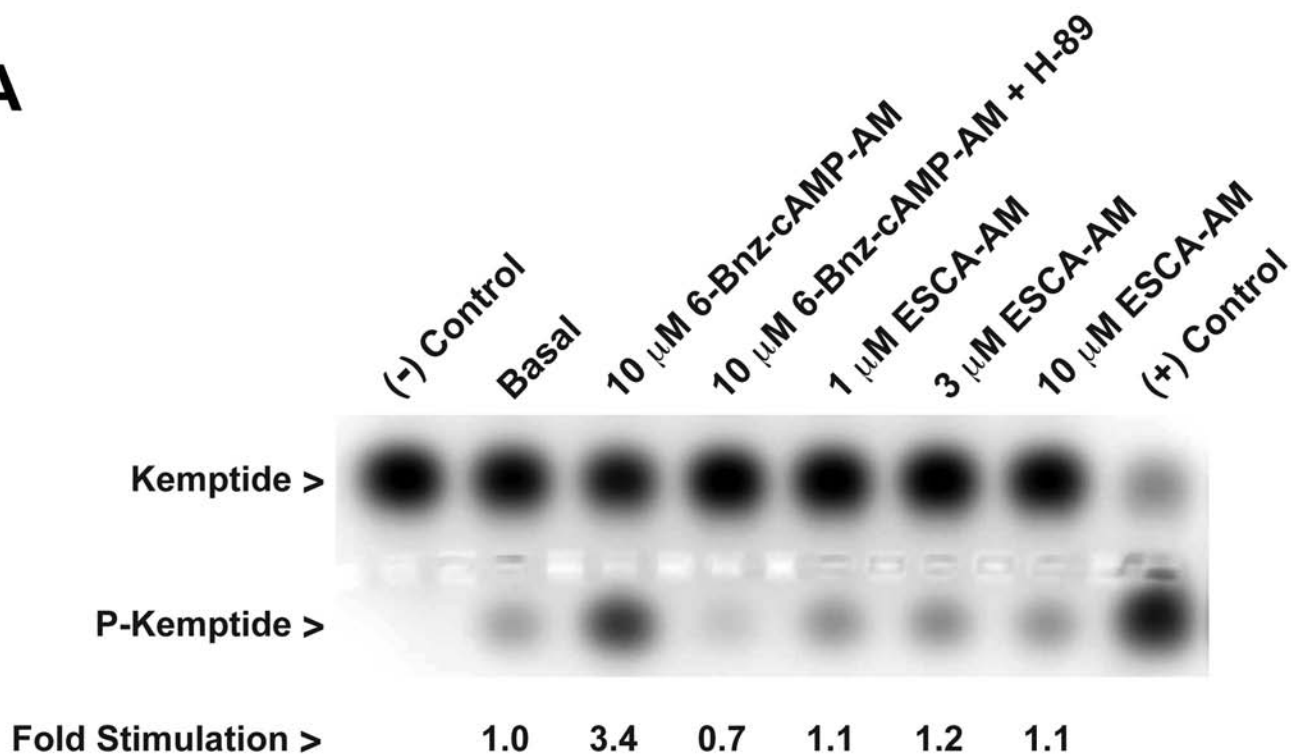
NP-EGTA-AM loaded mouse beta cells that were not subjected to UV flash photolysis, and that were bathed in SES that contained Ca<sup>2+</sup> (C) or did not contain Ca<sup>2+</sup> (D). E-F, under conditions of UV flash photolysis to uncage Ca<sup>2+</sup>, bafilomycin (1 μM) treated mouse beta cells did not exhibit CICR in the absence of 8-pCPT-2'-O-Me-cAMP-AM (E), but did exhibit CICR in the presence of 1 μM 8-pCPT-2'-O-Me-cAMP-AM (F). For each illustration, the horizontal bars indicate the time during which test substances were applied to individual cells using a glass puffer pipette. Findings are representative of 3 experiments using 10 cells for each treatment protocol.

**Figure 3. Western blot analysis of Epac2 expression in donor human islets**

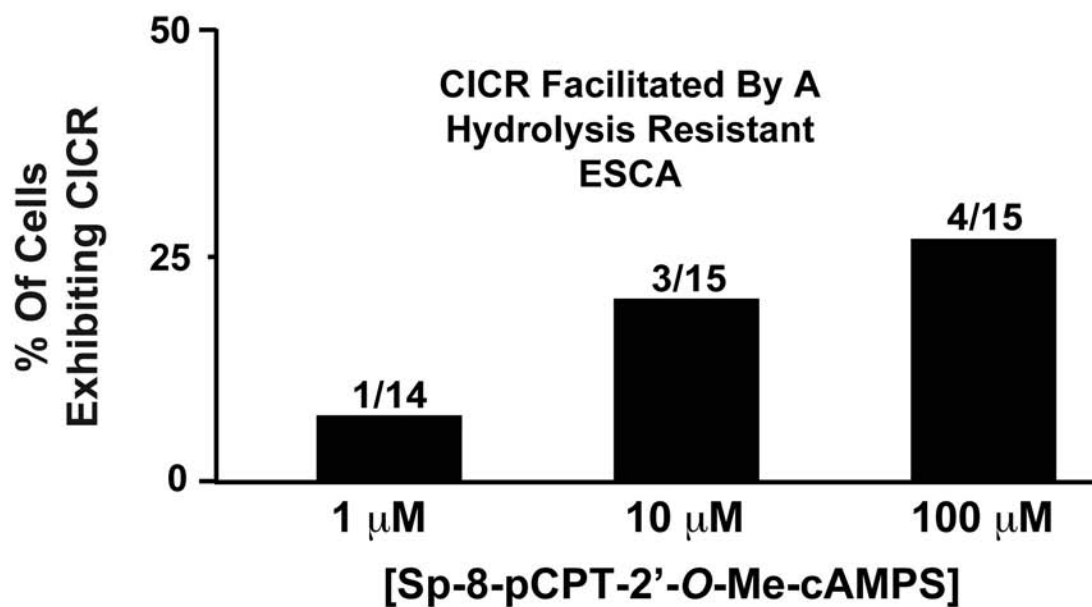
A, mouse monoclonal antibody (5B1) was used to detect recombinant Epac2 in lysates obtained from INS-1 cells overexpressing recombinant mouse Epac2 (*lane 1, positive control*). Immunoreactivity corresponding to endogenous Epac2 was also detected in human islets (*lane 2*), and this immunoreactivity exhibited a molecular mass (110 kDa) identical to that observed for recombinant Epac2. B, rabbit polyclonal antiserum Ab1536 was used to detect recombinant Epac2 in lysates obtained from INS-1 cells overexpressing recombinant mouse Epac2 (*lane 1*). These same lysates were processed with cAMP-conjugated agarose beads in order to “pull-down” recombinant Epac2, and a sample obtained from the pelleted lysate exhibited increased Epac2 immunoreactivity (*lane 2*), consistent with the fact that Epac2 is a cAMP-binding protein. For lysates of human islets not enriched using cAMP-conjugated agarose beads, Epac2 was still readily detectable using Ab1536 (*lane 3*).

# Supplemental Fig.1

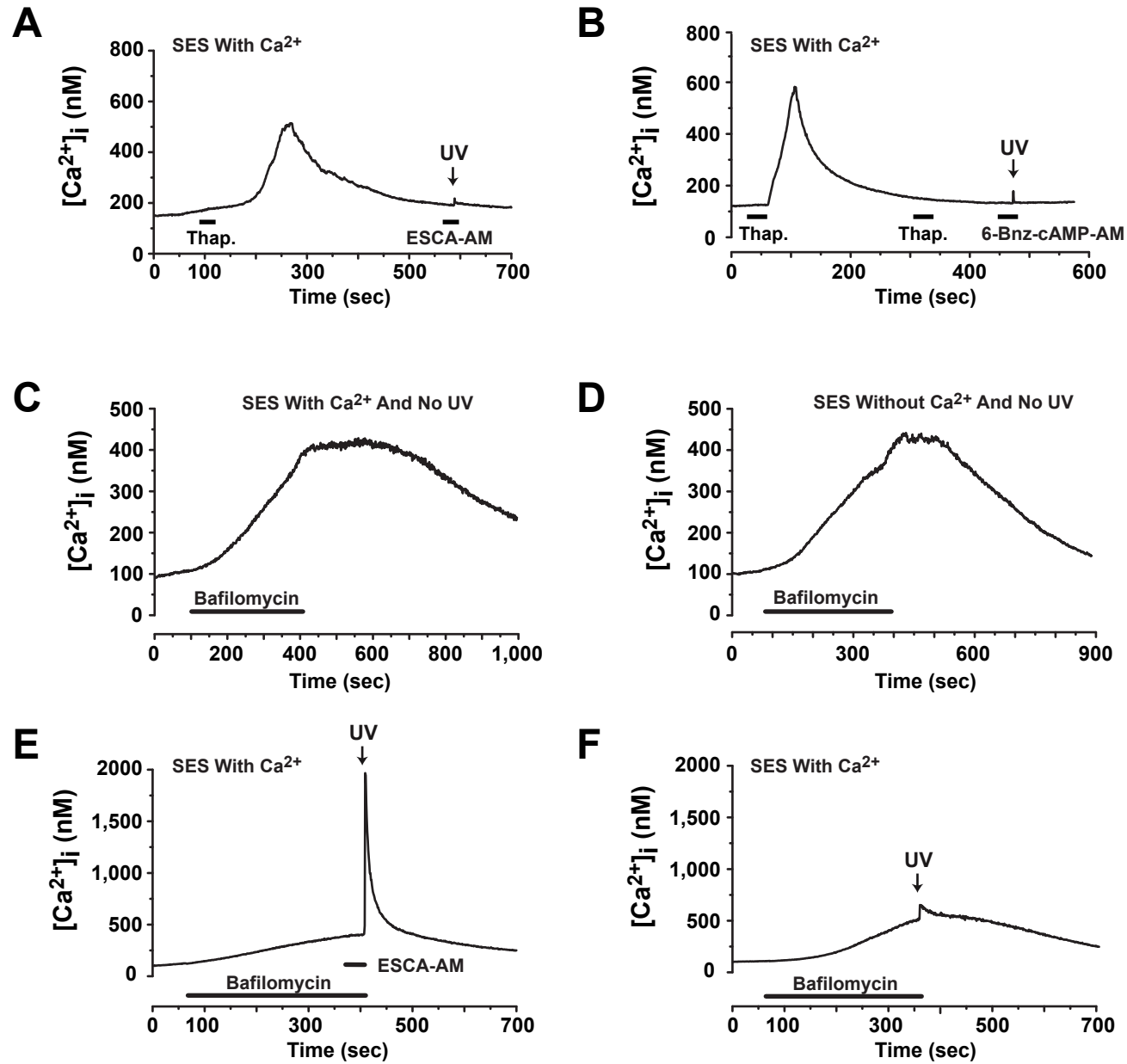
## A



## B



## Supplemental Fig.2



## Supplemental Fig.3

### Western Blot Analysis For Epac2

